PLASTID OSMOTIC STRESS INFLUENCES CELL DIFFERENTIATION AT THE PLANT SHOOT APEX

Margaret E. Wilson[1], Matthew Mixdorf[1], R. Howard Berg[2] and Elizabeth S. Haswell[1]*

[1]Department of Biology, Mailbox 1137, One Brookings Drive, Washington University in Saint Louis, Saint Louis, MO, USA 63130

[2]Donald Danforth Plant Science Center, 975 North Warson Rd., Saint Louis, MO, USA 63132

*Corresponding author

RUNNING TITLE

PLASTID STRESS AND CALLUS

SUMMARY STATEMENT

Plastid osmotic stress influences differentiation at the plant shoot apex. Two established mechanisms that control proliferation, the cytokinin/WUSCHEL stem cell identity loop and a plastid-to-nucleus signaling pathway, are implicated.

ABSTRACT

The balance between proliferation and differentiation in the plant shoot apical meristem is controlled by regulatory loops involving the phytohormone cytokinin and stem cell identity genes. Concurrently, cellular differentiation in the developing shoot is coordinated with the environmental and developmental status of plastids within those cells. Here we employ an *Arabidopsis thaliana* mutant exhibiting constitutive plastid osmotic stress to investigate the molecular and genetic pathways connecting plastid osmotic stress with cell differentiation at the shoot apex. *msl2 msl3* mutants exhibit dramatically enlarged and deformed plastids in the shoot apical meristem, and develop a mass of callus tissue at the shoot apex. Callus production in this mutant requires the cytokinin receptor AHK2 and is characterized by increased cytokinin levels, down-regulation of cytokinin signaling inhibitors ARR7 and ARR15, and induction of the stem cell identity gene *WUSCHEL*. Furthermore, plastid stress-induced apical callus production requires elevated plastidic ROS, ABA biosynthesis, the retrograde signaling protein GUN1, and ABI4. These results are consistent with a model wherein the cytokinin/WUS pathway and retrograde signaling control cell differentiation at the shoot apex.

36 **INTRODUCTION**

37

38 The development of land plants provides a unique opportunity to study how cell differentiation is
39 determined, as plant cell identity is highly plastic (Gaillochet and Lohmann, 2015). A classic illustration
40 of plant cell pluripotency is the ability to produce a mass of undifferentiated cells referred to as callus.
41 In nature, callus production is triggered by wounding or exposure to pathogens (Ikeuchi et al., 2013).
42 In the laboratory, callus is typically induced by exogenous treatment with two phytohormones,
43 cytokinin (CK) and auxin (Skoog and Miller, 1957).

44

45 Callus is frequently derived from meristem or meristem-like cells (Jiang et al., 2015; Sugimoto et al.,
46 2011). Meristems are small self-renewing pools of undifferentiated cells from which new organs are
47 derived as the plant grows (Aichinger et al., 2012; Gaillochet and Lohmann, 2015). Above ground, the
48 maintenance and regulation of the shoot apical meristem (SAM) is critical for the proper specification
49 and positioning of leaves (Barton, 2010). SAM identity requires both the imposition of stem cell fate by
50 the WUSCHEL(WUS)/CLAVATA(CLV) signaling circuit (Fletcher et al., 1999; Schoof et al., 2000) and
51 the suppression of differentiation by SHOOTMERISTEMLESS (STM) (Endrizzi et al., 1996; Long et al.,
52 1996).

53

54 CK plays a key role in the function of the SAM. In the central zone (CZ), CK promotes proliferation,
55 while auxin promotes differentiation in the peripheral zone (PZ) (Schaller et al., 2015). Localized CK
56 perception and response specifies the organizing center of the SAM, also the region of *WUS*
57 expression (Chickarmane et al., 2012; Gordon et al., 2009; Zurcher et al., 2013). WUS activity
58 maintains itself through a positive feedback loop involving CK response via Type-A Arabidopsis
59 Response Regulators (ARRs), key negative regulators of CK signaling (Leibfried et al., 2005; Schuster
60 et al., 2014; To et al., 2007; Zhao et al., 2010). In the SAM, auxin acts to repress *ARR7* and *ARR15*,
61 (Zhao et al., 2010). Thus, auxin and CK synergize to regulate the core WUS/CLV pathway,
62 maintaining a balance between differentiation and proliferation in the SAM (Gaillochet and Lohmann,
63 2015; Ikeuchi et al., 2013).

64

65 Shoot development also depends on plastids, endosymbiotic organelles responsible for
66 photosynthesis, amino acid, starch, and fatty acid biosynthesis and the production of many hormones
67 and secondary metabolites (Neuhaus and Emes, 2000). As cells leave the SAM and take on the
68 appropriate cell identity within leaf primordia, the small, undifferentiated plastids, called proplastids,
69 inside them must also differentiate, usually into chloroplasts. Many mutants lacking functional plastid-

70 localized proteins exhibit secondary defects in leaf cell specification ((Larkin, 2014; Luesse et al.,
71 2015; Moschopoulos et al., 2012), providing genetic evidence that normal leaf development depends
72 upon plastid homeostasis. The integration of plastid differentiation into the process of development
73 likely requires tightly regulated and finely tuned two-way communication between the plastid and the
74 nucleus, including both anterograde (nucleus-to-plastid) and retrograde (plastid-to-nucleus) signaling.
75 An increasing number of overlapping retrograde signaling pathways, triggered by developmental or
76 environmental defects in plastid function, have been identified (Chan et al., 2015; Woodson and Chory,
77 2012). Numerous retrograde signals have been proposed, including intermediates in isoprenoid (Xiao
78 et al., 2012) biosynthesis, heme (Woodson et al., 2011), phosphonucleotides (Estavillo et al., 2011),
79 reactive oxygen species (ROS) (Wagner et al., 2004) and oxidized carotenoids (Ramel et al., 2012).
80 Despite the diversity, all these pathways and signals link a disruption in plastid homeostasis to altered
81 nuclear gene expression (Chan et al., 2015).
82
83 One retrograde signaling pathway that may serve to connect plastid signals to shoot development is
84 the GENOMES UNCOUPLED (GUN1) / ABA-INSENSITIVE 4 (ABI4) pathway (Fernandez and Strand,
85 2008; Leon et al., 2012). ABI4 is a nuclear transcription factor involved in many plant developmental
86 pathways, including response to ABA, sugar signaling, and mitochondrial retrograde signaling (Leon et
87 al., 2012). GUN1 is a plastid protein of unclear molecular function thought to function with ABI4 in at
88 least two retrograde signaling pathways, one that coordinates plastid and nuclear gene expression
89 during development, and one that respond to defects in chlorophyll biosynthesis (Cottage et al., 2010;
90 Koussevitzky et al., 2007; Sun et al., 2011).
91
92 We have been using an Arabidopsis mutant with constitutively osmotically stressed plastids (*msl2*
93 *msl3* (Veley et al., 2012)) as a model system to address the developmental effects of plastid
94 dysfunction. MSL2 and MSL3 are two members of the MscS-Like family of mechanosensitive ion
95 channels that localize to the plastid envelope and are required for normal plastid size, shape, and
96 division site selection (Haswell and Meyerowitz, 2006; Wilson et al., 2011). By analogy to family
97 members in bacteria (Levina et al., 1999) and plants (Hamilton et al., 2015), and based on *in vivo*
98 experiments (Veley et al., 2012), MSL2 and MSL3 are likely to serve as osmotic “safety valves”,
99 allowing plastids to continuously maintain osmotic homeostasis during normal growth and
100 development. In addition, *msl2 msl3* mutant plants exhibit small stature, variegated leaf color, and
101 ruffled leaf margins. These whole-plant defects can be attributed to plastid osmotic stress, as they are
102 suppressed by environmental and genetic manipulations that increase cytoplasmic osmolarity and
103 draw water out of the plastid (Veley et al., 2012; Wilson et al., 2014). Here we report a new and

104 unexpected phenotype associated with *msl2 msl3* mutants, and establish the molecular and genetic
105 pathways that underlie it.

106 **RESULTS**

107

108 ***msl2 msl3* double mutants develop callus at the shoot apex**

109 When grown on solid media for over 14 days, *msl2 msl3* double mutant plants developed a
110 proliferating mass of undifferentiated cells, or callus, at the apex of the plant (Fig. 1A-D). A single
111 mass at the center of the apex, twin masses associated with the cotyledon petioles, or occasionally
112 three masses were observed Fig. 1A-C). New green tissue was frequently observed growing out of the
113 apical callus (white arrow, Fig. 1D). This phenotype was not observed in soil-grown plants.

114

115 Masses of callus tissue were apparent to the naked eye at the apex of *msl2 msl3* seedlings between
116 14 and 16 days after germination (DAG) and continued to grow in size through 22 DAG (Fig. 1E, top
117 two rows). As previously documented (Haswell and Meyerowitz, 2006; Jensen and Haswell, 2012;
118 Wilson et al., 2014), *msl2 msl3* leaves were small and malformed. To facilitate comparison, the same
119 leaf from each genotype is marked with an asterisk in the time course in Fig. 1E. The percent of *msl2*
120 *msl3* seedlings with callus increased to ~82% by 21 DAG (Fig. 1F); callus was not observed in any
121 wild type plants at any developmental stage.

122

123 We previously showed that growth on media containing increased levels of osmolytes (sugars or salt)
124 suppressed the plastid morphology and leaf development phenotypes of *msl2 msl3* mutants, likely by
125 increasing cytoplasmic osmolarity and reducing plastid hypoosmotic stress (Veley et al., 2012; Wilson
126 et al., 2014). To determine if the same were true for callus formation, and to assess the dependence
127 of suppression on age and developmental stage, seedlings were germinated on MS solid media and
128 transferred to media containing 82 mM NaCl at 2, 5, 7, or 9 DAG and assessed at 21 DAG for callus
129 formation and leaf development. Full suppression of callus formation and abnormal leaf development
130 was only observed in seedlings transferred to solid media containing NaCl from MS at 2 DAG (Fig.
131 1G-J), establishing a small developmental window after which alleviation of plastid hypoosmotic stress
132 can no longer suppress leaf morphology defects and apical callus production in *msl2 msl3* mutants.
133 Suppression was also observed when seedlings were grown on media containing sucrose, sorbitol or
134 mannitol, indicating that the effect is osmotic (Fig S1A.) The converse experiment, in which seedlings
135 were transferred from salt-containing media to normal MS showed that plastid osmotic homoeostasis
136 is continuously required to maintain normal leaf development (Fig. 1H and S1B).

137

138 **MSL2 function is required in the SAM or leaf primordia to prevent callus production**

139 To determine if MSL2 expression in the SAM and leaf primordia is required to prevent callus
140 production in the *msl2 msl3* background, we examined apical callus production in *msl2 msl3* mutant
141 plants expressing *MSL2* from the *SCARECROW (SCR)* promoter, which is expressed in the L1 cell
142 layer of the meristem and leaf primordia (Wysocka-Diller et al., 2000). As shown in Fig. 1H, apical
143 callus formation was fully suppressed in T2 *msl2 msl3 SCRpMSL2* lines. While these plants
144 developed multiple sets of developmentally normal true leaves, the majority of T2 lines examined
145 exhibited reduced stature.
146
147 **Cells and plastids at the apex of young *msl2 msl3* mutants are morphologically abnormal**
148 Closer examination of the apex of young (4-day-old) *msl2 msl3* mutant seedlings revealed a cluster of
149 disorganized and heterologously shaped cells with low electron density at the expected location of the
150 SAM (Fig 2A). Most cells within the cluster contained large, spherical, clear entities. In comparison,
151 the SAM cells of a wild type seedling were organized into cell layers and were electron-dense. We
152 next used transmission electron microscopy to further characterize the morphology of developing
153 chloroplasts and proplastids in the SAM and surrounding tissue of *msl2 msl3* mutant seedlings (Fig
154 2B). In the *msl2 msl3* mutant, young chloroplasts were enlarged, lacked the lens shape of wild-type
155 chloroplasts, and exhibited a disorganized developing thylakoid network (Fig. 2B-D and S2B). In
156 agreement with previous reports (Charuvi et al., 2012), wild-type proplastids appeared as small
157 structures (0.5-1 μm in diameter) containing rudimentary thylakoid networks of varying developmental
158 stages, plastoglobules, and double membranes (Fig. 2G and Fig. S2A). However, in the SAM of *msl2*
159 *msl3* mutants, entities with these established features had decreased stromal density and were greatly
160 enlarged compared to the wild type (asterisks in Fig. 2A and S2B, Fig. 2E). Many exceeded 5 μm in
161 diameter. All were clearly bound by a double membrane (white arrow, Fig. 2F and S2D-E). These data
162 show that the greatly enlarged phenotype of non-green plastids of the leaf epidermis (Haswell and
163 Meyerowitz, 2006; Veley et al., 2012) extends to proplastids of the SAM.
164
165 **Callus produced in *msl2 msl3* mutants is associated with an altered cytokinin: auxin ratio and**
166 **requires CK perception**
167 The production of shooty callus has been associated with increased production or availability of CKs
168 and an imbalance in the cytokinin: auxin ratio (Frank et al., 2002; Frank et al., 2000; Lee et al., 2004).
169 Consistent with these observations, apical callus production, dwarfing and leaf phenotypes of the *msl2*
170 *msl3* double mutant were strongly suppressed when seedlings were grown on media with the
171 synthetic auxin 1-naphthaleneacetic acid (NAA) (Fig. 3A, C). The leaf epidermis of *msl2 msl3*
172 seedlings contain grossly enlarged and round non-green plastids, as visualized with the fluorescent

173 plastid marker RecA-dsRED (Haswell and Meyerowitz, 2006; Veley et al., 2012; Wilson et al., 2014).
174 This phenotype was not altered by growth on 2 μM NAA (Fig. 3B), indicating that NAA treatment
175 suppresses callus formation downstream of effects on plastid morphology. In agreement with previous
176 data, growth on media supplemented with osmolytes fully suppressed the plastid morphology defects
177 (Veley et al., 2012). Trans-Zeatin-riboside levels were increased ~6.5-fold in *msl2 msl3* mutant
178 seedlings compared to the wild type, but IAA levels were not significantly changed (Fig. 3D).
179
180 The *ARABIDOPSIS HISTIDINE KINASE (AHK)2* gene encodes one of three related histidine kinases
181 known to function as CK receptors in Arabidopsis (Ueguchi et al., 2001; Yamada et al., 2001), and an
182 *AHK2* loss of function mutant, *ahk2-2* (Higuchi et al., 2004) is impaired in CK-induced up-regulation of
183 *WUS* (Gordon et al., 2009). Two independently isolated *msl2 msl3 ahk2-2* triple mutants showed a
184 significant reduction in apical callus formation with less than 40% of seedlings developing callus (Fig.
185 3F). However, the *msl2 msl3 ahk2-2* triple mutants were similar to the *msl2 msl3* double with respect
186 to leaf developmental defect (Fig. 3E). Incomplete suppression may be due to redundancy among CK
187 receptors (Gordon et al., 2009); or callus formation and leaf morphology defects may be produced
188 through different pathways.
189
190 To determine if feedback loops involving *WUS*, *ARRs* (Gordon et al., 2009; Schuster et al., 2014), or
191 the meristem identity gene *STM* (Scofield et al., 2013) were mis-regulated in *msl2 msl3* seedlings,
192 quantitative RT-PCR was used to determine transcript levels in the aerial tissue of 7- and 21-day-old
193 seedlings (Fig. 3G). In *msl2 msl3* mutant seedlings *WUS* transcript levels were up-regulated 5.3-fold
194 compared to the wild type by 7 DAG (prior to visible callus development, Fig. 1E); and 4-fold by 21
195 DAG. *STM* expression levels were up-regulated 2.1-fold in 7-day-old *msl2 msl3* mutants, but were not
196 distinguishable from the wild type at 21 DAG. Consistent with previous observations that they inhibit
197 callus formation (Buechel et al., 2010; Liu et al., 2016), *ARR7* and *ARR15* transcript levels were
198 reduced in both 7 and 21 day old *msl2 msl3* mutant seedlings compared to wild type, exhibiting 2 to
199 2.6-fold and 3- to 6-fold decreases, respectively. Transcriptional repression is specific to *ARR7* and
200 *ARR15* as transcript levels of two other A-type *ARR* genes, *ARR4* and *ARR5,* were elevated in *msl2*
201 *msl3* mutant seedlings compared to wild type. Hypocotyls from *msl2 msl3* mutants did not efficiently
202 produce callus in vitro, indicating that an additional signal or signals are required to produce callus
203 outside the SAM in these mutants (Fig. S3A). Furthermore, multiple genes involved in wound-inducible
204 and auxin-inducible callus production show altered expression in *msl2 msl3* mutants, including *WIND1*,
205 *WIND3*, *KPR2*, *KPR7*, *TSD1* and *TSD2* (Anzola et al., 2010; Frank et al., 2002; Iwase et al., 2011;
206 Krupkova and Schmulling, 2009) (Fig. S3B, C).

207

208 **Preventing Pro biosynthesis results in a dramatic increase in callus formation and CK levels in**
209 **the *msl2 msl3* background**

210 It was not obvious how the constitutive plastid osmotic stress experienced by *msl2 msl3* mutants might
211 elicit these effects, but we reasoned that the hyper-accumulation of solutes previously observed in
212 *msl2 msl3* mutants, especially the compatible osmolyte Proline (Pro) (Wilson et al., 2014), might be
213 responsible. To test this hypothesis, we crossed the *pyrroline-5-carboxylate synthetase1-1* (*p5cs1-4*)
214 lesion into the *msl2 msl3* mutant background. P5CS1 catalyzes the primary step in the inducible
215 production of Pro (Verslues and Sharma, 2010), and stress-induced Pro levels are low in this mutant
216 (Szekely et al., 2008). *msl2 msl3 p5cs1-4* triple mutant seedlings exhibited larger calluses than the
217 *msl2 msl3* double, frequently forming multiple calluses (Figs. 1E, and S4A), and formation was more
218 observed at earlier stages of development in *msl2 msl3 p5cs1-4* triple compared to *msl2 msl3* double
219 mutants (Fig. 4A, light blue bars)—at 14 DAG over 40% of triple mutant seedlings had visible callus,
220 while only 15% of the double *msl2 msl3* mutants did (Fig. 4A, light blue bars). Neither wild type nor
221 *p5cs1-4* single mutants produced callus at any time point. A different mutant allele of *P5CS1*, *p5cs1-1*
222 (Szekely et al., 2008), also enhanced callus formation in the *msl2 msl3* background (Fig. S4B-C). In
223 addition *msl2 msl3 p5cs1-4* triple mutants exhibited 7 times more trans-Zeatin-riboside levels than
224 *msl2 msl3* mutants (Fig. 3D). Supplementing growth media had no effect on callus production in *msl2*
225 *msl3* double or *msl2 msl3 p5cs1-4* triple mutants at any time point (Fig. 4A), even though *msl2 msl3*
226 *p5cs1-4* triple mutant seedlings grown on 20 mM Pro for 21 DAG contained as much Pro as the *msl2*
227 *msl3* double (Fig. 4B).

228

229 Thus, it is not the absence of Pro itself that leads to the enhanced callus production in the *msl2 msl3*
230 *p5cs1-4* triple mutants. Instead, disrupting the process of Pro biosynthesis could enhance callus
231 formation in the *msl2 msl3* mutant background if ROS accumulation were involved, as Pro
232 biosynthesis is a key reductive pathway that helps maintain cellular redox homeostasis (Szabados and
233 Savoure, 2010). To characterize the levels and localization of ROS in *msl2 msl3* double and *msl2 msl3*
234 *p5cs1-4* triple mutants, 7-, 14-, and 21-day-old mutant and wild-type seedlings were stained with 3, 3
235 diaminobenzidine (DAB) to detect hydrogen peroxide (H_2O_2) or nitroblue tetrazolium (NBT) to detect
236 superoxide (O_2^-) (Fig. 4C). Both double and triple mutants accumulated high levels of H_2O_2 and O_2^- in
237 the SAM region relative to the *p5cs1-4* single mutant or the wild type. Precipitate was visible earlier in
238 the *msl2 msl3 p5cs1-4* triple mutant (by 14 DAG compared to 21 DAG in the in the double *msl2 msl3*
239 mutant). Quantitation of H_2O_2 levels using an Amplex Red enzyme assay at these same time points
240 showed consistent accumulation of H_2O_2 in the double and triple mutants, rising to nearly three-fold

241 over wild type by 21 DAG (Fig. 4D). Levels of formazan, the product of NBT reduction by O_2^-,
242 increased in *msl2 msl3* and *msl2 msl3 p5cs1-4* to more than 2.5-fold above wild-type levels at 21 DAG
243 (Fig. 4E). Calluses generated by incubating *Arabidopsis thaliana* Col-*0* root explants on Callus
244 Inducing Media also showed strong NBT staining in areas of cell proliferation (Fig. S4), providing
245 evidence that ROS accumulation may be a general feature of callus tissue (Lee et al., 2004).
246
247 **The accumulation of superoxide in response to plastid hypo-osmotic stress is required for**
248 **callus formation in the *msl2 msl3* background.**
249 In plastids, the photoreduction of molecular O_2 generates O_2^-, which is then rapidly converted into
250 H_2O_2 by plastid-localized superoxide dismutase enzymes (Asada, 2006). To determine if plastid
251 osmotic stress and the accumulation of O_2^- at the apex of *msl2 msl3* double and *msl2 msl3 p5cs1-4*
252 triple mutants play causative roles in callus formation, plants were germinated on or transferred to
253 solid media with 82 mM NaCl or with TEMPOL (a O_2^- scavenger) at 3 or 7 DAG and stained with NBT
254 at 21 DAG. Growth on media containing NaCl suppressed O_2^- accumulation in *msl2 msl3* double and
255 *msl2 msl3 p5cs1-4* triple mutant seedlings (Fig. 5A), completely prevented callus formation (Fig. 5B),
256 suppressed defects in non-green plastid morphology (Fig. 5C) and leaf morphology (Fig. 5A). Thus,
257 plastid osmotic stress is responsible for O_2^- accumulation as well as callus formation in *msl2 msl3* and
258 *msl2 msl3 p5cs1-4* mutants. Consistent with Fig. 1H, growth on NaCl suppressed callus formation and
259 ROS accumulation only if supplied prior to 7 DAG.
260
261 Growth on TEMPOL-containing media successfully prevented the accumulation of O_2^- in the SAM of
262 *msl2 msl3* and *msl2 msl3 p5cs1-4* mutants, regardless of seedling age at time of application (Fig. 5A),
263 but did not affect plastid morphology (Fig, 5C) nor leaf morphology defects (Fig. 5A). Treating double
264 and triple mutant seedlings with TEMPOL at all developmental stages partially suppressed callus
265 formation (Fig. 5C). Less than 40% of double mutant seedlings exhibited apical calluses when grown
266 in the presence of TEMPOL, compared to > 90% when grown on MS without TEMPOL. TEMPOL-
267 mediated callus suppression is thus independent or downstream of the developmental window in
268 which addition of osmotic support must be provide for complete suppression of aerial phenotypes
269 (Figs 1H and 5A-B).
270
271 A complementary genetic approach to suppressing O_2^- accumulation in the plastid was taken by over-
272 expressing wild type or miR398-resistant forms of the chloroplast-localized Cu/Zn Superoxide
273 Dismutase CSD2 (Kliebenstein et al., 1998; Sunkar et al., 2006) in the *msl2 msl3* mutant background.
274 The percentage of seedlings with visible apical callus at 21 DAG was decreased to 50% or less in six

275 independent T2 lines segregating either wild-type (*CSD2*, lines #2, #4, and #7) or miR398 resistant
276 (*mCSD2*, lines #1, #3, #5) *CSD2* over-expression constructs (Fig. 5D). Approximately 50% of T2
277 seedlings showed strong O_2^- accumulation by NBT staining, which was localized to developing callus,
278 compared to 90% of *msl2 msl3* seedlings (Fig. 5E). 15-30% of seedlings in the CDS2 over-expression
279 lines exhibited both low levels of O_2^- accumulation at their shoot apex and did not develop callus; less
280 than 5% of *msl2 msl3* seedlings had these characteristics. Over-expression of *CSD2* did not suppress
281 abnormal leaf development (white arrows, Fig. 5F).
282
283 **Callus production requires ABA biosynthesis, ABI4 and GUN1**
284 As *msl2 msl3* double mutants exhibit increased levels of ABA and up-regulation of ABA biosynthesis
285 genes (Wilson et al., 2014), we hypothesized that a pathway involving the hormone ABA and the
286 *GUN1* and *ABI4* gene products might account for the pleiotropic defects in the *msl2 msl3* mutant
287 (Koussevitzky et al., 2007; Zhang et al., 2013). To determine if ABA biosynthesis was required for
288 callus production, we assessed the effect of introducing the *abscisic acid-deficient 2-1* allele (Schwartz
289 et al., 1997) on callus formation in the *msl2 msl3* background. Indeed, callus formation and leaf
290 development defects were strongly suppressed in a triple *msl2 msl3 aba2-1* mutant, with only ~20% of
291 seedlings developing callus at the shoot apex by 21 DAG (Fig. 6A, B). Similar suppression of *msl2*
292 *msl3* aerial defects was observed in four other independently isolated *msl2 msl3 aba2-1* triple mutant
293 lines. The *msl2 msl3 aba2-1* triple mutant accumulated trans-Zeatin-riboside to levels similar to the
294 *msl2 msl3* double mutant (Fig. 3D), suggesting that ABA and CK promote callus formation through
295 independent pathways.
296
297 To test if GUN1 is involved in the perception of signals generated by plastid osmotic stress, we
298 crossed the *gun1-9* (Koussevitzky et al., 2007) allele into the *msl2 msl3* mutant background and
299 analyzed the offspring of a single *msl2 msl3 gun1-2 (+/-)* mutant plant. Of twenty-seven triple *msl2*
300 *msl3 gun1-9* seedlings identified by PCR genotyping, none formed apical callus when grown on solid
301 media, whereas 16 of 19 genotyped sibling *msl2 msl3 gun1-9* (+/-) seedlings did. In
302 addition, *msl2 msl3 gun1-9* triple mutant siblings produced larger, greener, and more normally shaped
303 true leaves than their *msl2 msl3* and *msl2 msl3 gun1-9+/1* siblings (Fig. 6C, D). In some seedlings,
304 small and chlorotic true leaves developed at the seedling apex (Fig. 6E, S5).
305
306 The strong *abi4-1* allele (Finkelstein et al., 1998) was also introduced into the *msl2 msl3* background,
307 and *msl2 msl3 abi4-1* mutants also exhibited reduced apical callus formation; only ~26% of *msl2 msl3*
308 *abi4-1* seedlings from two independently isolated lines developed callus (Fig. 6F). Neither leaf

309 developmental defects nor ROS accumulation was suppressed in the *msl2 msl3 abi4-1* mutant, and
310 *msl2 msl3 abi4-1* seedlings stained with DAB or NBT showed a pattern of ROS accumulation similar
311 to the *msl2 msl3* double mutant (Fig. 6F, G). These staining patterns were not observed in wild type or
312 *abi4-1* single mutants. These results are consistent with a model wherein ABI4 functions downstream
313 of ROS accumulation, and likely in a pathway with GUN1, to induce apical callus formation in
314 response to plastid osmotic stress.
315

316 **DISCUSSION**

317

318 One of the most fundamental decisions a cell can make is whether to proliferate or to differentiate. In
319 the plant SAM, this decision must be spatially and temporally controlled, so that cells remain in an
320 undifferentiated, pluripotent state in the central zone of the meristem and then differentiate properly as
321 they are recruited into organs at the PZ. Here we use the *msl2 msl3* mutant as a model system to
322 show that, in the Arabidopsis SAM, proliferation versus differentiation signals are coordinated not only
323 at the tissue- and cellular-level, but also at the organellar level. We further applied genetic, molecular,
324 biochemical, and pharmacological approaches to identify two non-redundant pathways through which
325 plastid osmotic stress may produce apical callus (illustrated in Fig. S6).

326

327 **Plastid osmotic stress results in the production of callus at the plant SAM**

328 Plants lacking functional versions of the mechanosensitive ion channel homologs MSL2 and MSL3
329 robustly produce callus tissue at the apex of the plant when grown on solid media (Fig. 1). Molecular
330 complementation with *MSL2* under the control of the *SCARECROW* promoter established that
331 MSL2/MSL3 are required only in the L1 layer of the CZ and/or PZ of the SAM to prevent callus
332 formation (Fig. 2G) and that their function is critical during the first 5 days after germination (Fig 1G, H).
333 The production of apical callus in the *msl2 msl3* mutant is associated with dramatically enlarged and
334 developmentally abnormal plastids specifically in the SAM (Fig. 2A-F, S2A-D). Developmentally
335 defective plastids were also observed in the SAM of another apical callus-producing mutant, *tumorous*
336 *shoot development (tsd)1* (Frank et al., 2002).

337

338 **Increased proliferation and the production of callus in *msl2 msl3* mutants is associated with a**
339 **disruption in the CK/WUS feedback loop**

340 The *msl2 msl3* mutants exhibit several previously established hallmarks of increased proliferation at
341 the SAM, including increased levels of CK, up-regulation of the stem cell identity gene *WUSCHEL*,
342 and down-regulation of CK signaling inhibitors (Fig. 3D, G), suggesting that plastid osmotic stress
343 activates the CK/WUS feedback loop (Gaillochet et al., 2015; Ikeuchi et al., 2013) (top pathway, Fig.
344 S6). The resulting imbalance in the cytokinin: auxin ratio may underlie callus formation in the *msl2*
345 *msl3* background, as supplementing seedlings with exogenous auxin robustly suppresses all mutant
346 phenotypes (Fig. 3A, C) without affecting plastid osmotic stress (Fig 3B). In addition, the CK receptor
347 AHK2 is required for efficient callus formation (Fig. 3E, F). *AHK2* is required to maintain WUS
348 expression in the meristem in response to CK treatment in the CK/WUS feedback loop (Gordon et al.,

349 2009). Cytokinin and auxin are involved in the production of all types of callus (Perianez-Rodriguez et
350 al., 2014; Skoog and Miller, 1957), so alternative pathways to callus production cannot be ruled out.
351
352 Several previously identified callus-producing mutants in Arabidopsis and Helianthus also exhibit both
353 up-regulated CK signaling and defects in meristem identity gene expression, including *tsd1* (Frank et
354 al., 2002; Krupkova and Schmulling, 2009); EMB-2 (Chiappetta et al., 2006); and the *pasticcino*
355 mutants (Faure et al., 1998; Harrar et al., 2003). These data suggest that, the CK-induced pathway,
356 the wound-induced pathway and the meristematic identity pathway are interconnected pathways for
357 callus production. Furthermore, the *msl2 msl3* double mutant is the only callus-producing mutant
358 identified to date with a primary defect in plastid-localized proteins, adding a novel regulatory aspect to
359 these known pathways, and suggesting that plastid osmotic stress is uniquely able to trigger these
360 pathways. While we favor the model shown in Fig. S6, other interpretations are possible. Also
361 consistent with these data is a model wherein the *msl2 msl3* lesions lead to down-regulation of *TSD1*
362 and/or *TSD2*, or up-regulation of *WIND* genes, either of which could disrupt the CK/WUS loop.
363
364 **Plastid retrograde signaling is required for increased proliferation and the production of callus**
365 Genetic lesions that reduce Pro biosynthesis significantly exacerbated callus production in the *msl2*
366 *msl3* background, an effect that can not be attributed to low levels of Pro itself (Figs. 1E, 4A, B, S4).
367 Instead, the hyper-accumulation of ROS that results from blocking Pro biosynthesis is required (Fig. 5).
368 Treatment with exogenous ROS scavenger TEMPOL as well as over-production of CSD2, a
369 chloroplast-localized superoxide-scavenging enzyme, prevented or reduced callus formation. Plastid
370 osmotic stress was required for ROS hyper-accumulation (Fig. 5A-C). In addition, the analysis of
371 callus formation in higher order mutants established that ABA biosynthesis, the retrograde signaling
372 protein GUN1, and the transcription factor ABI4 were required for callus formation and act
373 downstream of ROS (Fig. 6, bottom pathway in Fig. S6). Because we were able to specifically
374 suppress callus production, ROS accumulation, and impaired leaf development by increasing
375 cytoplasmic osmolarity in the *msl2 msl3* background, this phenotype is very unlikely to be due to a
376 loss of specific signaling by MSL2 or MSL3.
377
378 Multiple genetic links between plastid function and cell differentiation in the shoot have been
379 previously described, and are often cited as evidence for retrograde signaling (Inaba and Ito-Inaba,
380 2010; Lepisto and Rintamaki, 2012; Lundquist et al., 2014). ROS accumulation has been documented
381 in at least one other callus-producing mutant, *tsd2*/*quasimodo2* (Raggi et al., 2015). Whether ROS
382 and/or an ABA/GUN1/ABI4 retrograde signaling pathway are employed to communicate plastid

383 dysfunction to shoot development in any of these other mutants is not known. However, the
384 application of pharmacological inhibitors of plastid development or function was used to demonstrate
385 that leaf adaxial/abaxial patterning is regulated by plastid protein translation in a GUN1-dependent
386 pathway (Tameshige et al., 2013), and the GUN1 pathway is required to facilitate the switch from leaf
387 cell proliferation to expansion and differentiation (Andriankaja et al., 2012). Taken together with the
388 results reported here, these data support previously proposed models wherein a variety of plastid
389 dysfunctions are communicated to leaf development through similar or overlapping pathways that
390 include GUN1 (Koussevitzky et al., 2007; Leon et al., 2012). ABI4 may function with GUN1 in this
391 retrograde signaling pathway, or the reduction in *msl2 msl3* callus production in the *abi4-1* mutant
392 background may result from indirect effects on sugar signaling or ABA biosynthesis.
393
394 We note that only a few of the genetic or pharmacological treatments that suppressed callus formation
395 in the *msl2 msl3* mutant also suppressed the leaf developmental defects. Growth on exogenous auxin
396 was the only treatment to completely suppress all of the mutant phenotypes, while preventing CK
397 signaling, ABA biosynthesis, ROS accumulation, GUN1, or ABI4 function only partially rescued leaf
398 defects (Figs. 3E-F, 6A-E). It is possible that these differences are due to genetic redundancy or to
399 limited uptake or transport of TEMPOL. Alternatively, there may be two fundamentally different
400 processes that respond to plastid osmotic stress in the *msl2 msl3* mutant: one that functions in the
401 SAM during early development, and one that functions later on in the leaves. In support of the latter
402 proposal, subjecting seedlings to mild hyperosmotic stress has been shown to prevent leaf cell
403 proliferation (Skirycz et al., 2011).
404
405 ***msl2 msl3* mutants may provide a functional link between the CK/WUS feedback loop and**
406 **plastid retrograde signaling in controlling cell differentiation at the plant apex.**
407 Our working model, illustrated in Fig. S6, is that the production of apical callus in *msl2 msl3* mutants
408 operates through two non-redundant pathways: the CK/WUS feedback loop and a retrograde signaling
409 pathway involving ROS, ABA, ABI4 and GUN1. While the data presented here establish that both of
410 these pathways are required for callus formation in the *msl2 msl3* background, whether they operate
411 completely independently or are interconnected is not yet clear. Here we present them as separate
412 pathways; support for this comes from the fact that CK levels remain elevated in the *aba2 msl2 msl3*
413 triple mutant (Fig. 3D), indicating that ABA biosynthesis is not upstream of the CK/WUS feedback loop.
414 Furthermore, mutants that solely overproduce plastid ROS (Myouga et al., 2008) up-regulate CK
415 signaling (To et al., 2004), or hyper-accumulate Pro (Mattioli et al., 2008) have not been reported to
416 produce apical callus, implying that a combination of these signals is required.

We speculate that two-way communication between plastids and cell differentiation is essential to coordinate the developmental and functional state of the plastid with that of the cell within which it resides, and that it therefore necessarily involves multiple pathways. These results add yet another layer of complexity to the many regulatory pathways and feedback loops that govern dynamic cell identity decision-making at the plant shoot apex, and provide a foundation for future investigation into the relationship between meristem identity and plastid osmotic homeostasis in the SAM.

424 **MATERIALS AND METHODS**

425

426 ***Arabidopsis thaliana* Mutants**

427 The *aba2-1* (CS156), *abi4-1* (CS8104), *p5cs1-4* (SALK_063517), *p5cs1-1* (SALK_058000), *ahk2-2*
428 (SALK_052531), *gun1-9*, and *msl2-3* alleles are in the Columbia-*0* background. The *msl3-1* allele is in
429 the Wassilewskija background (Haswell and Meyerowitz, 2006). Derived cleaved-amplified
430 polymorphic sequence genotyping (Neff et al., 1998) of the *gun1-9* allele was performed using oligos
431 CGAACGACGAAAGATTGTGAGGAGGGTCT and CCTGCAAGCATTCAGAATCGCTGAAAAAGG,
432 digesting with PstI. The *abi4-1* allele was genotyped with oligos TCAATCCGATTCCACCACCGAC
433 and CCACTTCCTCCTTGTTCCTGC, digesting with NlaI. PCR genotyping of *msl*, *p5cs1*, and *aba2-1*
434 alleles was performed as previously described (Sharma and Verslues, 2010; Szekely et al., 2008;
435 Wilson et al., 2011).

436

437 **Plant Growth**

438 Plants were grown on full-strength Murashige and Skoog (MS) medium (pH 5.7; Caisson Labs) with
439 0.8% (w/v) agar (Caisson Labs). NaCl, L-Pro (Sigma) and TEMPOL (Sigma) were added before
440 autoclaving. For transfer assays, seed was surface-sterilized, sown on nylon mesh strips overlaid on
441 1X MS or 1X MS + 82 mM NaCl, and stratified for 2 d at 4°C before growth and transfer as described.
442 All plants were grown at 23°C under a 16 h light regime, 130-160 μmol m^{-1} s^{-1}.

443

444 **Microscopy**

445 Confocal microscopy of ds-RED labeled non-green plastids was performed as in (Wilson et al., 2014).
446 Bright-field images were captured with an Olympus DP71 microscope digital camera and processed
447 with DP-BSW software. Apical meristems were ultra-rapidly frozen in a Baltec high- pressure freezer
448 (Bal-Tec HPM010), excluding air with packing buffer (75 mM PIPES, pH 6.8, 50 mM
449 sucrose). Samples were freeze substituted in 2% osmium/ acetone at -85°C for five days, slowly
450 thawed to 25°C over 16 hours, and embedded in Spurrs resin. One μm sections for phase microscopy
451 were stained 30 seconds with 1% Toluidine Blue O in 1% boric acid. Transmission electron
452 microscopy was done on thin sections of tissue fixed for 2 h in 2% glutaraldehyde, post-fixed 90
453 minutes in 2% osmium tetroxide and embedded in Spurr's resin. Sections were stained in uranyl and
454 lead salts.

455

456 **ROS Detection and Quantification**

457 Detection of H_2O_2 using 3,3'-Diaminobenzidine (DAB, Sigma) was performed as described (Wu et al.,
458 2012) with the following modifications. Whole seedlings were incubated for 2 hrs in 1 mg/ml DAB prior
459 to vacuum infiltration, incubated in the dark for an additional 12 hrs, then cleared with an ethanol
460 series. An Amplex Red Hydrogen Peroxide/Peroxidase Assay Kit (Invitrogen) was used to measure
461 H_2O_2 production in seedlings. For in vitro localization of O_2^- with Nitrotetrazolium Blue chloride (NBT;
462 Sigma), whole seedlings were vacuum-infiltrated with 0.1% (w/v) NBT in a 10 mM potassium
463 phosphate buffer (pH 7.8) containing 10 mM NaN_3. After 1-hour incubation in the dark at RT seedlings
464 were cleared with an ethanol series. Quantification of formazan levels was performed as described in
465 (Myouga et al., 2008).
466
467 **Subcloning and Transgenic lines**
468 pENTR-MSL2 (Haswell and Meyerowitz, 2006) was used in a Gateway technology (Life Technologies)
469 recombination reaction with pSCR:GW (Michniewicz et al., 2015) to create *pSCR:MSL2*.
470
471 **Quantitative Reverse Transcription-PCR**
472 Quantitative reverse transcription-PCR was performed as previously described (Wilson et al., 2011).
473 Primers used for gene expression analysis of *ACTIN* and *ARR* genes were previously described
474 (Wilson et al., 2014; Zhao et al., 2010). The following primer pairs were used to amplify *WUS*
475 (GCGATGCTTATCTGGAACAT and CTTCCAGATGGCACCACTAC) and *STM*
476 (CAAATGGCCTTACCCTTCG and GCCGTTTCCTCTGGTTTATG).
477
478 **ACKNOWLEDGEMENTS**
479 We thank Kelsey Kropp, Jeffrey Berry and the Proteomics and Mass Spectrometry Facility of the
480 Donald Danforth Plant Science Center for technical assistance, Lucia Strader for *abi4-1* seeds and
481 pSCR:GW, Ramanjulu Sunkar for pBIB-CSD2 and pBIB-mCSD2;,and Joanne Chory for *gun1-9* seeds.
482 This research was funded by NSF MCB-1253103 and NASA NNX13AM55G.
483
484 **COMPETING INTERESTS**
485 No competing interests declared.
486
487 **AUTHOR CONTRIBUTIONS**
488 Study conception and manuscript preparation, MEW, ESH; conducting research and formal analysis,
489 MEW, RHB, MM; funding acquisition, ESH.
490

491 **FIGURE LEGENDS**

492

493 **Fig. 1. *msl2 msl3* double mutants develop callus at the shoot apex.** (A-D) Bright-field images of
494 21-day-old *msl2 msl3* seedlings grown on solid media. Shooty callus is indicated with a white
495 arrowhead in (D). (E) Time course of callus formation. (F) Average percent of *msl2 msl3* seedlings
496 with visible callus at the indicated time after germination. Five plates of seedlings, n > 10 seedlings per
497 plate, were analyzed per time point. (G) 21-day-old seedlings scored in (H) (top) or seedlings
498 transferred from MS with 82 mM NaCl to MS at indicated time points (bottom). (H) The average
499 percent of *msl2 msl3* seedlings showing visible callus at 21 DAG after transfer from MS to MS (black
500 bars) or from MS to MS with 82 mM NaCl (grey bars) at the indicated time points. 3 plates of seedlings,
501 n > 10 seedlings per plate, were analyzed per treatment. Error bars indicate SEM. *, difference
502 between indicated samples, $P < 0.01$ (Student's *t*-test). (I-M) Close-up images of individual seedlings
503 shown in (G) grown without NaCl (I) or transferred to NaCl plates at 2 (J), 5 (K), or 7 (L) DAG. (M)
504 Bright-field images of 14-day-old *msl2 msl3* seedlings harboring the *MSL2* transgene (*MSL2g*) or
505 *MSL2* under the control of the *SCR* promoter. Size bars (A-E), 1 mm, (G, M), 5 mm, (I-L), 2.5 mm.

506

507 **Fig. 2. Four-day-old *msl2 msl3* mutants exhibit abnormal cellular organization and plastids at**
508 **the SAM.** (A) Phase contrast images of the SAM region of seedlings of the indicated genotypes. Size
509 bar, 50 μm. (B-G) Transmission electron microscope (TEM) images of *msl2 msl3* mutant SAM (B) and
510 developing chloroplasts (C-D) and proplastids (E-F) in wild type and *msl2 msl3* mutant seedlings. (G)
511 Magnified region of *msl2 msl3* plastid envelope, indicated by box in F. Examples of proplastids and
512 developing chloroplasts are indicated in *msl2 msl3* mutant by asterisks and black arrowheads,
513 respectively. Size bar, 10 μm (B-D), 1 μm (E), and 100 nm (F-G). Plastoglobules (PG), double
514 membrane (white arrowheads), and thylakoids (double black arrowheads) are indicated.

515

516 **Fig. 3. Callus produced in *msl2 msl3* mutants is associated with increased CK production and**
517 **requires CK signaling.** (A) Seedlings grown for 21 days on solid media containing the indicated
518 concentration of NAA. Size bar, 1 mm. (B) Confocal micrographs of non-green plastids in the first true
519 leaf of *msl2 msl3* mutants harboring the RecA-dsRED plastid marker and grown on indicated media.
520 Size bar, 10 μm. (C) Percent of *msl2 msl3* mutants exhibiting callus when grown on NAA. The average
521 of three biological replicates of ≥ 20 seedlings each is presented. Statistical groups were determined
522 by ANOVA followed by Tukey's HSD test, $P < 0.01$. (D) Trans-Zeatin-riboside and IAA levels of 21-
523 day-old seedlings determined by liquid chromatography-mass spectrometry/mass spectrometry
524 analysis as in (Chen et al., 2009). The average of three biological replicates of ≥ 30 seedlings each is

525 presented. Error bars indicate SD, *, difference from wild type, $P < 0.01$ (Student's *t*-test). Images of
526 seedlings (E) and callus production rates (F) of *msl2 msl3 ahk2-2* triple mutant and parental lines. Size
527 bar, 1 mm. White arrows mark deformed leaves. The average of four biological replicates of ≥ 20
528 seedlings each is presented. Error bars indicate SEM. *, difference from *msl2 msl3*, $P < 0.01$
529 (Student's *t*-test). (G) Quantitative RT-PCR analysis of gene expression in the *msl2 msl3* mutant. The
530 average of three biological replicates (two technical replicates; n ≥ 25 seedlings each) is presented.
531 Error bars indicate SEM, asterisks indicate difference from wild type of same age, **P ≤ 0.05, **P ≤
532 0.01 (Student's *t*-test).
533
534 **Fig. 4. Preventing Pro biosynthesis results in a dramatic increase in callus formation in the**
535 ***msl2 msl3* background. (**A) Production of apical callus in *msl2 msl3* and *msl2 msl3 p5cs1-4*
536 seedlings in the presence and absence of exogenously provided Pro. The average of three biological
537 replicates is presented, $n \geq 25$ seedlings each. Error bars represent SD. *, difference from *msl2 msl3*
538 seedlings of the same age, $P < 0.01$ (Student's *t*-test). (B) Pro content of the aerial tissue of mutant
539 and wild-type seedlings grown as in (A), measured as in (Wilson et al., 2014). The average of two
540 biological replicates (each performed in triplicate; n ≥ 30 seedlings each) is presented. (C) Images of
541 the meristematic region of seedlings stained with DAB or NBT. Size bar, 1 mm. Quantification of H_2O_2
542 content by Amplex Red (D) and O_2^- production by NBT-Formazan production (E) in mutant and wild-
543 type seedlings of indicated age. The average of three biological replicates ($n \geq 20$ seedlings each),
544 two technical replicates each, is presented in both (D) and (E). Statistical grouping in (B), (D), and (E)
545 was performed as in Fig. 3C, and error bars indicate SEM**.** FW, fresh weight.
546
547 **Fig. 5. Hyper-accumulation of superoxide is required for callus formation in *msl2 msl3* and**
548 ***msl2 msl3 p5cs1* seedlings.** (A) NBT stained seedlings provided with TEMPOL or NaCl at 0, 3 or 7
549 DAG. Size bar, 1mm. (B) Callus production in mutant seedlings when grown on MS, MS with 1 mM
550 TEMPOL or MS with 82 mM NaCl. (C) Confocal micrographs of non-green plastids in the first true leaf
551 of *msl2 msl3* mutants harboring the RecA-dsRED plastid marker grown on the indicated media. Size
552 bar, 10 μm. (D) Apical callus production in T2 lines segregating transgenes that over-express *CSD2* or
553 *mCSD2*. The average of 4 biological replicates ($n \geq 35$ seedlings each replicate) is presented. Error
554 bars indicate SD. Statistical grouping was performed as in Fig. 3C. (E) Percent of seedlings from (D)
555 stained with NBT accumulating formazan at the shoot apex. ($n \geq 20$ seedlings). (F) Images of *CSD2*
556 over-expression T2 lines. Size bar, 1 mm. White arrows mark deformed leaves.
557

558 **Fig. 6. Callus production requires ABA biosynthesis, GUN1 and ABI4.** (A) 21-day-old *msl2 msl3*
559 double and *msl2 msl3 aba2-1* triple mutant seedlings. (B) Callus production in higher order mutants at
560 21 DAG. The average of 3 biological replicates ($n \geq 15$ seedlings per replicate) is presented. Error
561 bars indicate SEM. (C-D) 21-day-old *msl2 msl3 gun1-9* (+/-) (C) and *msl2 msl3 gun1-9* (-/-) (D, E)
562 siblings at 21 DAG. (F) 21-day-old *msl2 msl3 abi4-1* seedlings with relevant parental controls. (G) 21-
563 day-old seedlings of the indicated genotypes stained with DAB or NBT. (A, F, G) Size bar, 1 mm. (C,
564 D, E) Size bar, 2.5 cm.
565
566

567 **REFERENCES**

568

569 **Aichinger, E., Kornet, N., Friedrich, T. and Laux, T.** (2012). Plant stem cell niches. *Annual Review*
570 *of Plant Biology* **63**, 615-636.

571 **Andriankaja, M., Dhondt, S., De Bodt, S., Vanhaeren, H., Coppens, F., De Milde, L., Muhlenbock,**
572 **P., Skirycz, A., Gonzalez, N., Beemster, G. T., et al.** (2012). Exit from proliferation during leaf
573 development in Arabidopsis thaliana: a not-so-gradual process. *Developmental Cell* **22**, 64-78.

574 **Anzola, J. M., Sieberer, T., Ortbauer, M., Butt, H., Korbei, B., Weinhofer, I., Mullner, A. E. and**
575 **Luschnig, C.** (2010). Putative Arabidopsis transcriptional adaptor protein (PROPORZ1) is
576 required to modulate histone acetylation in response to auxin. *Proceedings of the National*
577 *Academy of Sciences of the United States of America* **107**, 10308-10313.

578 **Asada, K.** (2006). Production and scavenging of reactive oxygen species in chloroplasts and their
579 functions. *Plant Physiology* **141**, 391-396.

580 **Barton, M. K.** (2010). Twenty years on: the inner workings of the shoot apical meristem, a
581 developmental dynamo. *Dev Biol* **341**, 95-113.

582 **Buechel, S., Leibfried, A., To, J. P., Zhao, Z., Andersen, S. U., Kieber, J. J. and Lohmann, J. U.**
583 (2010). Role of A-type ARABIDOPSIS RESPONSE REGULATORS in meristem maintenance
584 and regeneration. *Eur J Cell Biol* **89**, 279-284.

585 **Chan, K. X., Phua, S. Y., Crisp, P., McQuinn, R. and Pogson, B. J.** (2015). Learning the Languages
586 of the Chloroplast: Retrograde Signaling and Beyond. *Annual Review of Plant Biology* **67**, 25-
587 53.

588 **Charuvi, D., Kiss, V., Nevo, R., Shimoni, E., Adam, Z. and Reich, Z.** (2012). Gain and loss of
589 photosynthetic membranes during plastid differentiation in the shoot apex of Arabidopsis. *The*
590 *Plant Cell* **24**, 1143-1157.

591 **Chen, Q., Zhang, B., Hicks, L. M., Wang, S. and Jez, J. M.** (2009). A liquid chromatography-tandem
592 mass spectrometry-based assay for indole-3-acetic acid-amido synthetase. *Anal Biochem* **390**,
593 149-154.

594 **Chiappetta, A., Michelotti, V., Fambrini, M., Bruno, L., Salvini, M., Petrarulo, M., Azmi, A., Van**
595 **Onckelen, H., Pugliesi, C. and Bitonti, M. B.** (2006). Zeatin accumulation and misexpression
596 of a class I knox gene are intimately linked in the epiphyllous response of the interspecific
597 hybrid EMB-2 (Helianthus annuus x H. tuberosus). *Planta* **223**, 917-931.

598 **Chickarmane, V. S., Gordon, S. P., Tarr, P. T., Heisler, M. G. and Meyerowitz, E. M.** (2012).
599 Cytokinin signaling as a positional cue for patterning the apical-basal axis of the growing

600 Arabidopsis shoot meristem. *Proceedings of the National Academy of Sciences of the United*
601 *States of America* **109**, 4002-4007.
602 **Cottage, A., Mott, E. K., Kempster, J. A. and Gray, J. C.** (2010). The Arabidopsis plastid-signalling
603 mutant gun1 (genomes uncoupled1) shows altered sensitivity to sucrose and abscisic acid and
604 alterations in early seedling development. *Journal of Experimental Botany* **61**, 3773-3786.
605 **Endrizzi, K., Moussian, B., Haecker, A., Levin, J. Z. and Laux, T.** (1996). The SHOOT
606 MERISTEMLESS gene is required for maintenance of undifferentiated cells in Arabidopsis
607 shoot and floral meristems and acts at a different regulatory level than the meristem genes
608 WUSCHEL and ZWILLE. *The Plant Journal* **10**, 967-979.
609 **Estavillo, G. M., Crisp, P. A., Pornsiriwong, W., Wirtz, M., Collinge, D., Carrie, C., Giraud, E.,**
610 **Whelan, J., David, P., Javot, H., et al.** (2011). Evidence for a SAL1-PAP chloroplast
611 retrograde pathway that functions in drought and high light signaling in Arabidopsis. *The Plant*
612 *Cell* **23**, 3992-4012.
613 **Faure, J. D., Vittorioso, P., Santoni, V., Fraisier, V., Prinsen, E., Barlier, I., Van Onckelen, H.,**
614 **Caboche, M. and Bellini, C.** (1998). The PASTICCINO genes of Arabidopsis thaliana are
615 involved in the control of cell division and differentiation. *Development* **125**, 909-918.
616 **Fernandez, A. P. and Strand, A.** (2008). Retrograde signaling and plant stress: plastid signals initiate
617 cellular stress responses. *Curr Opin Plant Biol* **11**, 509-513.
618 **Finkelstein, R. R., Wang, M. L., Lynch, T. J., Rao, S. and Goodman, H. M.** (1998). The Arabidopsis
619 abscisic acid response locus ABI4 encodes an APETALA 2 domain protein. *The Plant Cell* **10**,
620 1043-1054.
621 **Fletcher, J. C., Brand, U., Running, M. P., Simon, R. and Meyerowitz, E. M.** (1999). Signaling of
622 cell fate decisions by CLAVATA3 in Arabidopsis shoot meristems. *Science* **283**, 1911-1914.
623 **Frank, M., Guivarc'h, A., Krupkova, E., Lorenz-Meyer, I., Chriqui, D. and Schmulling, T.** (2002).
624 Tumorous shoot development (TSD) genes are required for co-ordinated plant shoot
625 development. *The Plant Journal* **29**, 73-85.
626 **Frank, M., Rupp, H. M., Prinsen, E., Motyka, V., Van Onckelen, H. and Schmulling, T.** (2000).
627 Hormone autotrophic growth and differentiation identifies mutant lines of Arabidopsis with
628 altered cytokinin and auxin content or signaling. *Plant Physiology* **122**, 721-729.
629 **Gaillochet, C., Daum, G. and Lohmann, J. U.** (2015). O cell, where art thou? The mechanisms of
630 shoot meristem patterning. *Curr Opin Plant Biol* **23**, 91-97.
631 **Gaillochet, C. and Lohmann, J. U.** (2015). The never-ending story: from pluripotency to plant
632 developmental plasticity. *Development* **142**, 2237-2249.

633 **Gordon, S. P., Chickarmane, V. S., Ohno, C. and Meyerowitz, E. M.** (2009). Multiple feedback
634 loops through cytokinin signaling control stem cell number within the Arabidopsis shoot
635 meristem. *Proceedings of the National Academy of Sciences of the United States of America*
636 **106**, 16529-16534.
637 **Hamilton, E. S., Jensen, G. S., Maksaev, G., Katims, A., Sherp, A. M. and Haswell, E. S.** (2015).
638 Mechanosensitive channel MSL8 regulates osmotic forces during pollen hydration and
639 germination. *Science* **350**, 438-441.
640 **Harrar, Y., Bellec, Y., Bellini, C. and Faure, J. D.** (2003). Hormonal control of cell proliferation
641 requires PASTICCINO genes. *Plant Physiology* **132**, 1217-1227.
642 **Haswell, E. S. and Meyerowitz, E. M.** (2006). MscS-like proteins control plastid size and shape in
643 Arabidopsis thaliana. *Current Biology : CB* **16**, 1-11.
644 **Higuchi, M., Pischke, M. S., Mahonen, A. P., Miyawaki, K., Hashimoto, Y., Seki, M., Kobayashi,**
645 **M., Shinozaki, K., Kato, T., Tabata, S., et al.** (2004). In planta functions of the Arabidopsis
646 cytokinin receptor family. *Proceedings of the National Academy of Sciences of the United*
647 *States of America* **101**, 8821-8826.
648 **Ikeuchi, M., Sugimoto, K. and Iwase, A.** (2013). Plant callus: mechanisms of induction and
649 repression. *The Plant Cell* **25**, 3159-3173.
650 **Inaba, T. and Ito-Inaba, Y.** (2010). Versatile roles of plastids in plant growth and development. *Plant*
651 *& Cell Physiology* **51**, 1847-1853.
652 **Iwase, A., Mitsuda, N., Koyama, T., Hiratsu, K., Kojima, M., Arai, T., Inoue, Y., Seki, M.,**
653 **Sakakibara, H., Sugimoto, K., et al.** (2011). The AP2/ERF transcription factor WIND1
654 controls cell dedifferentiation in Arabidopsis. *Current Biology : CB* **21**, 508-514.
655 **Jensen, G. S. and Haswell, E. S.** (2012). Functional analysis of conserved motifs in the
656 mechanosensitive channel homolog MscS-Like2 from Arabidopsis thaliana. *PloS one* **7**,
657 e40336.
658 **Jiang, F., Feng, Z., Liu, H. and Zhu, J.** (2015). Involvement of Plant Stem Cells or Stem Cell-Like
659 Cells in Dedifferentiation. *Frontiers in Plant Science* **6**, 1028.
660 **Kliebenstein, D. J., Monde, R. A. and Last, R. L.** (1998). Superoxide dismutase in Arabidopsis: an
661 eclectic enzyme family with disparate regulation and protein localization. *Plant Physiology* **118**,
662 637-650.
663 **Koussevitzky, S., Nott, A., Mockler, T. C., Hong, F., Sachetto-Martins, G., Surpin, M., Lim, J.,**
664 **Mittler, R. and Chory, J.** (2007). Signals from chloroplasts converge to regulate nuclear gene
665 expression. *Science* **316**, 715-719.

666 **Krupkova, E. and Schmulling, T.** (2009). Developmental consequences of the tumorous shoot
667 development1 mutation, a novel allele of the cellulose-synthesizing KORRIGAN1 gene. *Plant*
668 *Molecular Biology* **71**, 641-655.
669 **Larkin, R. M.** (2014). Influence of plastids on light signalling and development. *Philosophical*
670 *Transactions of the Royal Society of London* **369**, 20130232.
671 **Lee, J. H., Kim, D. M., Lim, Y. P. and Pai, H. S.** (2004). The shooty callus induced by suppression of
672 tobacco CHRK1 receptor-like kinase is a phenocopy of the tobacco genetic tumor. *Plant Cell*
673 *Rep* **23**, 397-403.
674 **Leibfried, A., To, J. P., Busch, W., Stehling, S., Kehle, A., Demar, M., Kieber, J. J. and Lohmann,**
675 **J. U.** (2005). WUSCHEL controls meristem function by direct regulation of cytokinin-inducible
676 response regulators. *Nature* **438**, 1172-1175.
677 **Leon, P., Gregorio, J. and Cordoba, E.** (2012). ABI4 and its role in chloroplast retrograde
678 communication. *Frontiers in Plant Science* **3**, 304.
679 **Lepisto, A. and Rintamaki, E.** (2012). Coordination of plastid and light signaling pathways upon
680 development of Arabidopsis leaves under various photoperiods. *Molecular Plant* **5**, 799-816.
681 **Levina, N., Totemeyer, S., Stokes, N. R., Louis, P., Jones, M. A. and Booth, I. R.** (1999).
682 Protection of Escherichia coli cells against extreme turgor by activation of MscS and MscL
683 mechanosensitive channels: identification of genes required for MscS activity. *The EMBO*
684 *Journal* **18**, 1730-1737.
685 **Liu, Z., Li, J., Wang, L., Li, Q., Lu, Q., Yu, Y., Li, S., Bai, M. Y., Hu, Y. and Xiang, F.** (2016).
686 Repression of callus initiation by the miRNA-directed interaction of auxin-cytokinin in
687 Arabidopsis thaliana. *The Plant Journal* [Epub ahead of print].
688 **Long, J. A., Moan, E. I., Medford, J. I. and Barton, M. K.** (1996). A member of the KNOTTED class
689 of homeodomain proteins encoded by the STM gene of Arabidopsis. *Nature* **379**, 66-69.
690 **Luesse, D. R., Wilson, M. E. and Haswell, E. S.** (2015). RNA Sequencing Analysis of the msl2msl3,
691 crl, and ggps1 Mutants Indicates that Diverse Sources of Plastid Dysfunction Do Not Alter Leaf
692 Morphology Through a Common Signaling Pathway. *Frontiers in Plant Science* **6**, 1148.
693 **Lundquist, P. K., Rosar, C., Brautigam, A. and Weber, A. P.** (2014). Plastid signals and the bundle
694 sheath: mesophyll development in reticulate mutants. *Molecular Plant* **7**, 14-29.
695 **Mattioli, R., Marchese, D., D'Angeli, S., Altamura, M. M., Costantino, P. and Trovato, M.** (2008).
696 Modulation of intracellular proline levels affects flowering time and inflorescence architecture in
697 Arabidopsis. *Plant Molecular Biology* **66**, 277-288.
698 **Michniewicz, M., Frick, E. M. and Strader, L. C.** (2015). Gateway-compatible tissue-specific vectors
699 for plant transformation. *BMC Res Notes* **8**, 63.

700 **Moschopoulos, A., Derbyshire, P. and Byrne, M. E.** (2012). The Arabidopsis organelle-localized
701 glycyl-tRNA synthetase encoded by EMBRYO DEFECTIVE DEVELOPMENT1 is required for
702 organ patterning. *Journal of Experimental Botany* **63**, 5233-5243.
703 **Myouga, F., Hosoda, C., Umezawa, T., Iizumi, H., Kuromori, T., Motohashi, R., Shono, Y., Nagata,**
704 **N., Ikeuchi, M. and Shinozaki, K.** (2008). A heterocomplex of iron superoxide dismutases
705 defends chloroplast nucleoids against oxidative stress and is essential for chloroplast
706 development in Arabidopsis. *The Plant Cell* **20**, 3148-3162.
707 **Neff, M. M., Neff, J. D., Chory, J. and Pepper, A. E.** (1998). dCAPS, a simple technique for the
708 genetic analysis of single nucleotide polymorphisms: experimental applications in Arabidopsis
709 thaliana genetics. *The Plant Journal* **14**, 387-392.
710 **Neuhaus, H. E. and Emes, M. J.** (2000). Nonphotosynthetic Metabolism in Plastids. *Annu Rev Plant*
711 *Physiol Plant Mol Biol* **51**, 111-140.
712 **Perianez-Rodriguez, J., Manzano, C. and Moreno-Risueno, M. A.** (2014). Post-embryonic
713 organogenesis and plant regeneration from tissues: two sides of the same coin? *Frontiers in*
714 *Plant Science* **5**, 219.
715 **Raggi, S., Ferrarini, A., Delledonne, M., Dunand, C., Ranocha, P., De Lorenzo, G., Cervone, F.**
716 **and Ferrari, S.** (2015). The Arabidopsis Class III Peroxidase AtPRX71 Negatively Regulates
717 Growth under Physiological Conditions and in Response to Cell Wall Damage. *Plant*
718 *Physiology* **169**, 2513-2525.
719 **Ramel, F., Birtic, S., Ginies, C., Soubigou-Taconnat, L., Triantaphylides, C. and Havaux, M.**
720 (2012). Carotenoid oxidation products are stress signals that mediate gene responses to
721 singlet oxygen in plants. *Proceedings of the National Academy of Sciences of the United*
722 *States of America* **109**, 5535-5540.
723 **Schaller, G. E., Bishopp, A. and Kieber, J. J.** (2015). The yin-yang of hormones: cytokinin and auxin
724 interactions in plant development. *The Plant Cell* **27**, 44-63.
725 **Schoof, H., Lenhard, M., Haecker, A., Mayer, K. F., Jurgens, G. and Laux, T.** (2000). The stem cell
726 population of Arabidopsis shoot meristems in maintained by a regulatory loop between the
727 CLAVATA and WUSCHEL genes. *Cell* **100**, 635-644.
728 **Schuster, C., Gaillochet, C., Medzihradszky, A., Busch, W., Daum, G., Krebs, M., Kehle, A. and**
729 **Lohmann, J. U.** (2014). A regulatory framework for shoot stem cell control integrating
730 metabolic, transcriptional, and phytohormone signals. *Developmental Cell* **28**, 438-449.
731 **Schwartz, S. H., Leon-Kloosterziel, K. M., Koornneef, M. and Zeevaart, J. A.** (1997). Biochemical
732 characterization of the aba2 and aba3 mutants in Arabidopsis thaliana. *Plant Physiology* **114**,
733 161-166.

734 **Scofield, S., Dewitte, W., Nieuwland, J. and Murray, J. A.** (2013). The Arabidopsis homeobox gene
735 SHOOT MERISTEMLESS has cellular and meristem-organisational roles with differential
736 requirements for cytokinin and CYCD3 activity. *The Plant Journal* **75**, 53-66.
737 **Sharma, S. and Verslues, P. E.** (2010). Mechanisms independent of abscisic acid (ABA) or proline
738 feedback have a predominant role in transcriptional regulation of proline metabolism during low
739 water potential and stress recovery. *Plant, Cell & Environment* **33**, 1838-1851.
740 **Skirycz, A., Claeys, H., De Bodt, S., Oikawa, A., Shinoda, S., Andriankaja, M., Maleux, K., Eloy,**
741 **N. B., Coppens, F., Yoo, S. D., et al.** (2011). Pause-and-stop: the effects of osmotic stress on
742 cell proliferation during early leaf development in Arabidopsis and a role for ethylene signaling
743 in cell cycle arrest. *The Plant Cell* **23**, 1876-1888.
744 **Skoog, F. and Miller, C. O.** (1957). Chemical regulation of growth and organ formation in plant
745 tissues cultured in vitro. *Symp Soc Exp Biol* **11**, 118-130.
746 **Sugimoto, K., Gordon, S. P. and Meyerowitz, E. M.** (2011). Regeneration in plants and animals:
747 dedifferentiation, transdifferentiation, or just differentiation? *Trends Cell Biol* **21**, 212-218.
748 **Sun, X., Feng, P., Xu, X., Guo, H., Ma, J., Chi, W., Lin, R., Lu, C. and Zhang, L.** (2011). A
749 chloroplast envelope-bound PHD transcription factor mediates chloroplast signals to the
750 nucleus. *Nat Commun* **2**, 477.
751 **Sunkar, R., Kapoor, A. and Zhu, J. K.** (2006). Posttranscriptional induction of two Cu/Zn superoxide
752 dismutase genes in Arabidopsis is mediated by downregulation of miR398 and important for
753 oxidative stress tolerance. *The Plant Cell* **18**, 2051-2065.
754 **Szabados, L. and Savoure, A.** (2010). Proline: a multifunctional amino acid. *Trends Plant Sci* **15**, 89-
755 97.
756 **Szekely, G., Abraham, E., Cseplo, A., Rigo, G., Zsigmond, L., Csiszar, J., Ayaydin, F., Strizhov,**
757 **N., Jasik, J., Schmelzer, E., et al.** (2008). Duplicated P5CS genes of Arabidopsis play distinct
758 roles in stress regulation and developmental control of proline biosynthesis. *The Plant Journal*
759 **53**, 11-28.
760 **Tameshige, T., Fujita, H., Watanabe, K., Toyokura, K., Kondo, M., Tatematsu, K., Matsumoto, N.,**
761 **Tsugeki, R., Kawaguchi, M., Nishimura, M., et al.** (2013). Pattern dynamics in adaxial-
762 abaxial specific gene expression are modulated by a plastid retrograde signal during
763 Arabidopsis thaliana leaf development. *PLoS Genet* **9**, e1003655.
764 **To, J. P., Deruere, J., Maxwell, B. B., Morris, V. F., Hutchison, C. E., Ferreira, F. J., Schaller, G. E.**
765 **and Kieber, J. J.** (2007). Cytokinin regulates type-A Arabidopsis Response Regulator activity
766 and protein stability via two-component phosphorelay. *The Plant Cell* **19**, 3901-3914.

767 **To, J. P., Haberer, G., Ferreira, F. J., Deruere, J., Mason, M. G., Schaller, G. E., Alonso, J. M.,**
768 **Ecker, J. R. and Kieber, J. J.** (2004). Type-A Arabidopsis response regulators are partially
769 redundant negative regulators of cytokinin signaling. *The Plant Cell* **16**, 658-671.
770 **Ueguchi, C., Koizumi, H., Suzuki, T. and Mizuno, T.** (2001). Novel family of sensor histidine kinase
771 genes in Arabidopsis thaliana. *Plant & Cell Physiology* **42**, 231-235.
772 **Veley, K. M., Marshburn, S., Clure, C. E. and Haswell, E. S.** (2012). Mechanosensitive channels
773 protect plastids from hypoosmotic stress during normal plant growth. *Current Biology : CB* **22**,
774 408-413.
775 **Verslues, P. E. and Sharma, S.** (2010). Proline metabolism and its implications for plant-environment
776 interaction. *The Arabidopsis book / American Society of Plant Biologists* **8**, e0140.
777 **Wagner, D., Przybyla, D., Op den Camp, R., Kim, C., Landgraf, F., Lee, K. P., Wursch, M., Laloi,**
778 **C., Nater, M., Hideg, E., et al.** (2004). The genetic basis of singlet oxygen-induced stress
779 responses of Arabidopsis thaliana. *Science* **306**, 1183-1185.
780 **Wilson, M. E., Basu, M. R., Bhaskara, G. B., Verslues, P. E. and Haswell, E. S.** (2014). Plastid
781 osmotic stress activates cellular stress responses in Arabidopsis. *Plant Physiology* **165**, 119-
782 128.
783 **Wilson, M. E., Jensen, G. S. and Haswell, E. S.** (2011). Two mechanosensitive channel homologs
784 influence division ring placement in Arabidopsis chloroplasts. *The Plant Cell* **23**, 2939-2949.
785 **Woodson, J. D. and Chory, J.** (2012). Organelle signaling: how stressed chloroplasts communicate
786 with the nucleus. *Current Biology : CB* **22**, R690-692.
787 **Woodson, J. D., Perez-Ruiz, J. M. and Chory, J.** (2011). Heme synthesis by plastid ferrochelatase I
788 regulates nuclear gene expression in plants. *Current Biology : CB* **21**, 897-903.
789 **Wu, A., Allu, A. D., Garapati, P., Siddiqui, H., Dortay, H., Zanor, M. I., Asensi-Fabado, M. A.,**
790 **Munne-Bosch, S., Antonio, C., Tohge, T., et al.** (2012). JUNGBRUNNEN1, a reactive
791 oxygen species-responsive NAC transcription factor, regulates longevity in Arabidopsis. *The*
792 *Plant Cell* **24**, 482-506.
793 **Wysocka-Diller, J. W., Helariutta, Y., Fukaki, H., Malamy, J. E. and Benfey, P. N.** (2000).
794 Molecular analysis of SCARECROW function reveals a radial patterning mechanism common
795 to root and shoot. *Development* **127**, 595-603.
796 **Xiao, Y., Savchenko, T., Baidoo, E. E., Chehab, W. E., Hayden, D. M., Tolstikov, V., Corwin, J. A.,**
797 **Kliebenstein, D. J., Keasling, J. D. and Dehesh, K.** (2012). Retrograde signaling by the
798 plastidial metabolite MEcPP regulates expression of nuclear stress-response genes. *Cell* **149**,
799 1525-1535.

800 **Yamada, H., Suzuki, T., Terada, K., Takei, K., Ishikawa, K., Miwa, K., Yamashino, T. and Mizuno,**
801 **T.** (2001). The Arabidopsis AHK4 histidine kinase is a cytokinin-binding receptor that
802 transduces cytokinin signals across the membrane. *Plant & Cell Physiology* **42**, 1017-1023.
803 **Zhang, Z. W., Feng, L. Y., Cheng, J., Tang, H., Xu, F., Zhu, F., Zhao, Z. Y., Yuan, M., Chen, Y. E.,**
804 **Wang, J. H., et al.** (2013). The roles of two transcription factors, ABI4 and CBFA, in ABA and
805 plastid signalling and stress responses. *Plant Molecular Biology* **83**, 445-458.
806 **Zhao, Z., Andersen, S. U., Ljung, K., Dolezal, K., Miotk, A., Schultheiss, S. J. and Lohmann, J. U.**
807 (2010). Hormonal control of the shoot stem-cell niche. *Nature* **465**, 1089-1092.
808 **Zurcher, E., Tavor-Deslex, D., Lituiev, D., Enkerli, K., Tarr, P. T. and Muller, B.** (2013). A robust
809 and sensitive synthetic sensor to monitor the transcriptional output of the cytokinin signaling
810 network in planta. *Plant Physiology* **161**, 1066-1075.
811
812

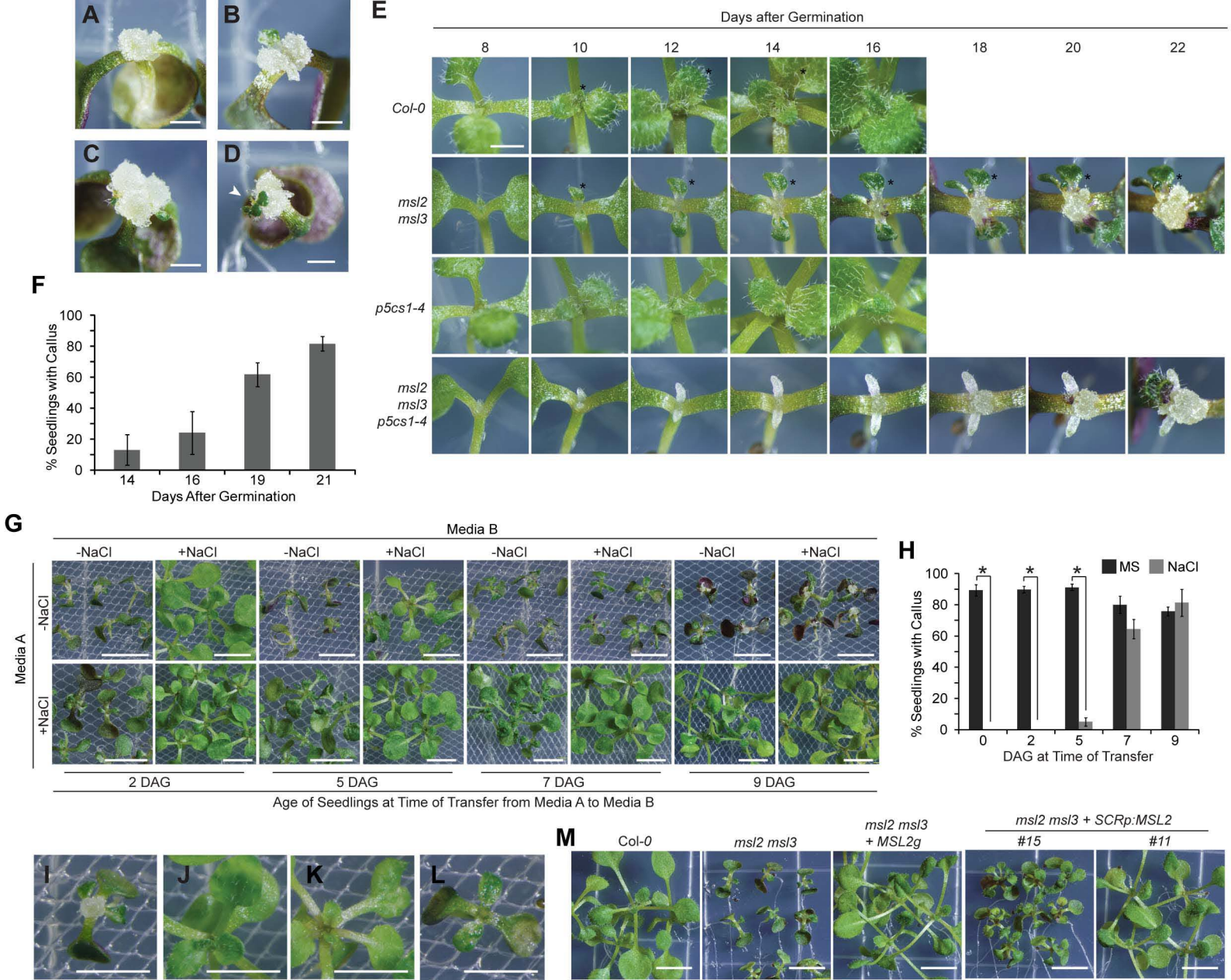
A
B
C
D
E
Days after Germination
8
10
12
14
16
18
20
22
Col-0
msl2
msl3
p5cs1-4
msl2
msl3
p5cs1-4
F
% Seedlings with Callus
100
80
60
40
20
0
14
16
19
21
Days After Germination
G
Media B
-NaCl
+NaCl
-NaCl
+NaCl
-NaCl
+NaCl
-NaCl
+NaCl
Media A
-NaCl
+NaCl
2 DAG
5 DAG
7 DAG
9 DAG
Age of Seedlings at Time of Transfer from Media A to Media B
H
MS
NaCl
% Seedlings with Callus
100
80
60
40
20
0
0
2
5
7
9
DAG at Time of Transfer
I
J
K
L
M
Col-0
msl2 msl3
msl2 msl3
+ MSL2g
msl2 msl3 + SCRp:MSL2
#15
#11

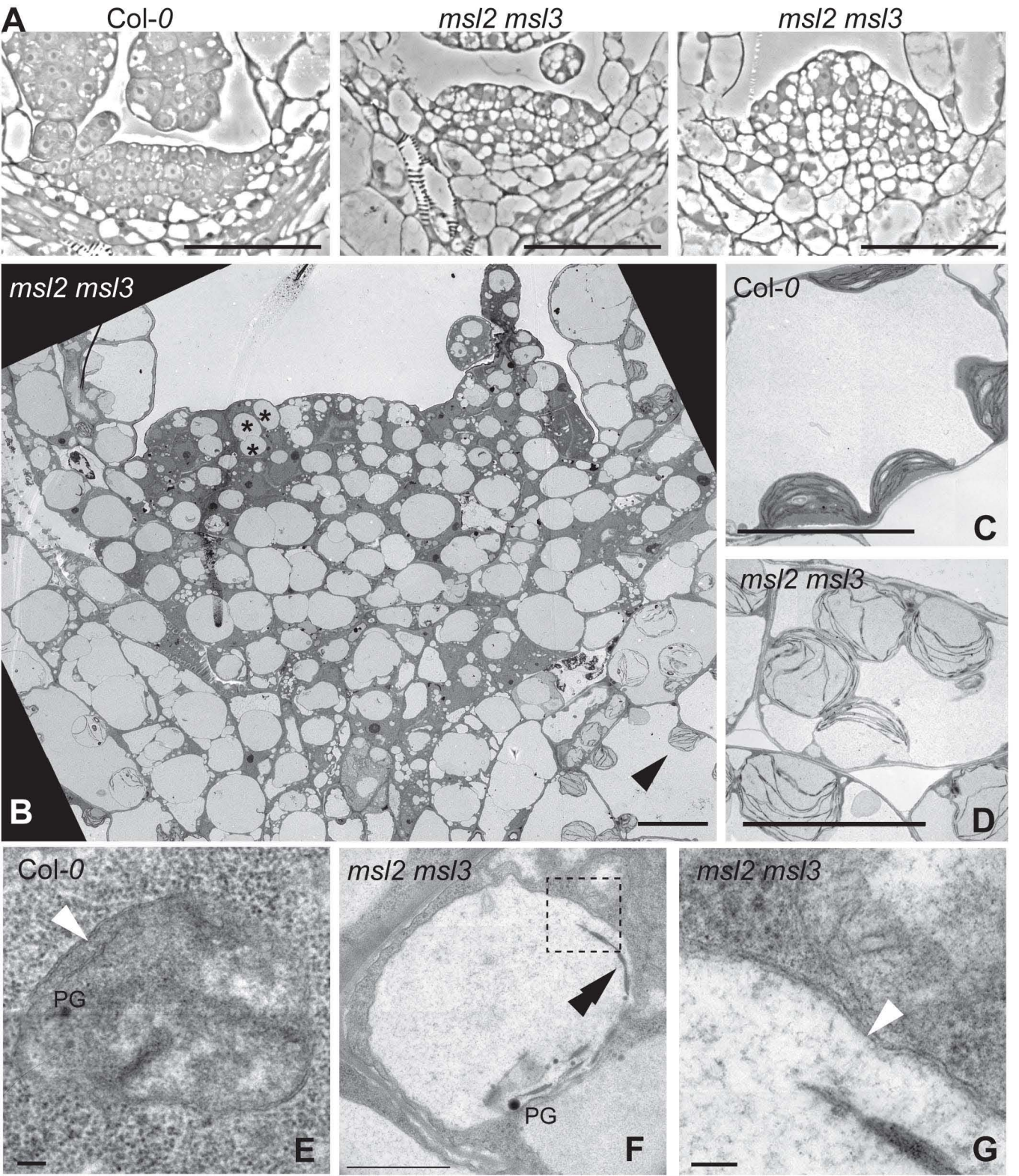
A
Col-0
msl2 msl3
msl2 msl3
msl2 msl3
B
Col-0
C
msl2 msl3
D
Col-0
PG
E
msl2 msl3
PG
F
msl2 msl3
G

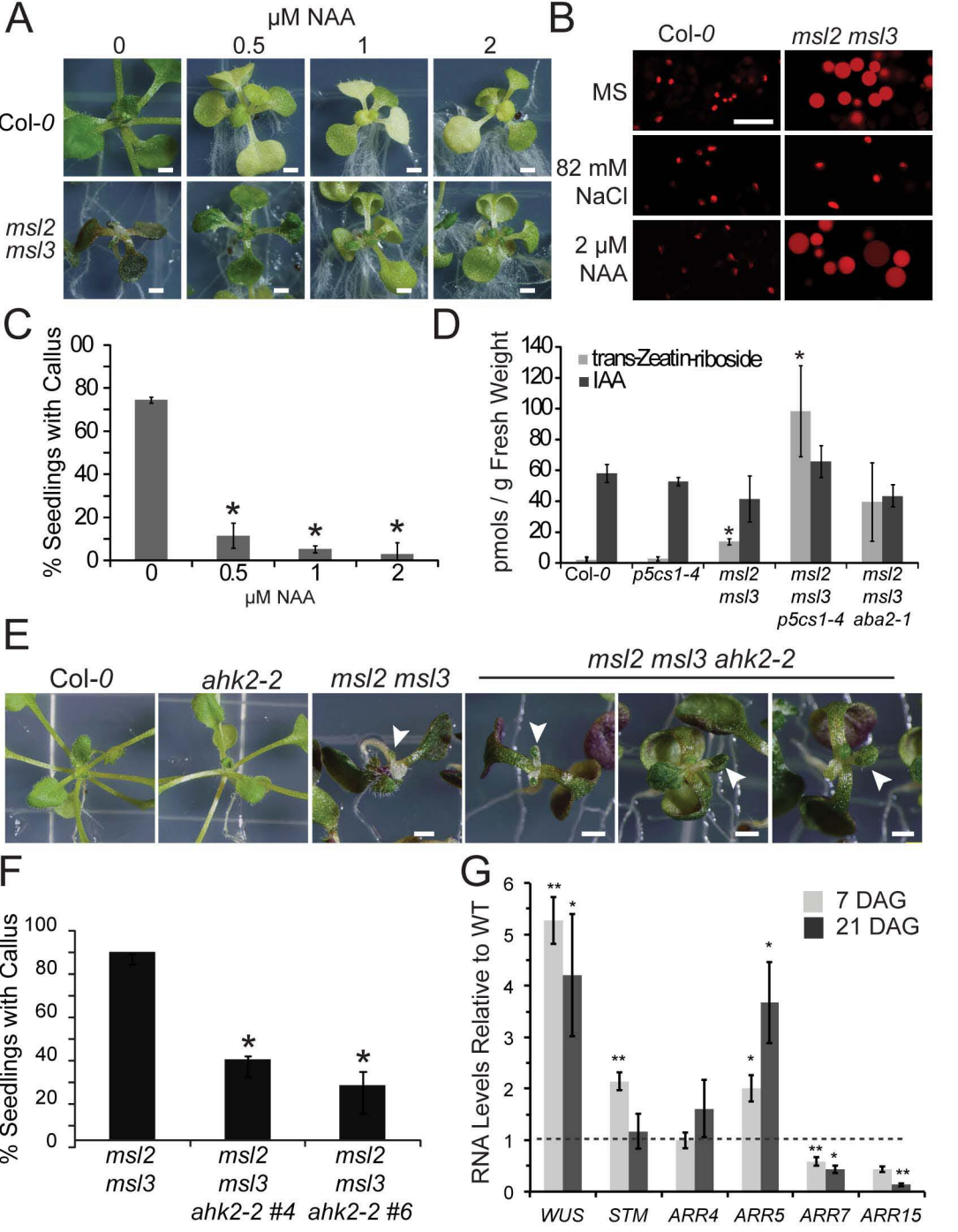
A
μM NAA
0
0.5
1
2
Col-0
msl2 msl3
B
Col-0
msl2 msl3
MS
82 mM NaCl
2 μM NAA
C
% Seedlings with Callus
00
80
60
40
20
0
0
0.5
1
2
μM NAA
D
pmols / g Fresh Weight
140
120
100
80
60
40
20
0
trans-Zeatin-riboside
IAA
Col-0
p5cs1-4
msl2 msl3
msl2 msl3 p5cs1-4
msl2 msl3 aba2-1
E
Col-0
ahk2-2
msl2 msl3
msl2 msl3 ahk2-2
F
% Seedlings with Callus
100
80
60
40
20
0
msl2 msl3
msl2 msl3 ahk2-2 #4
msl2 msl3 ahk2-2 #6
G
RNA Levels Relative to WT
6
5
4
3
2
1
0
7 DAG
21 DAG
WUS
STM
ARR4
ARR5
ARR7
ARR15

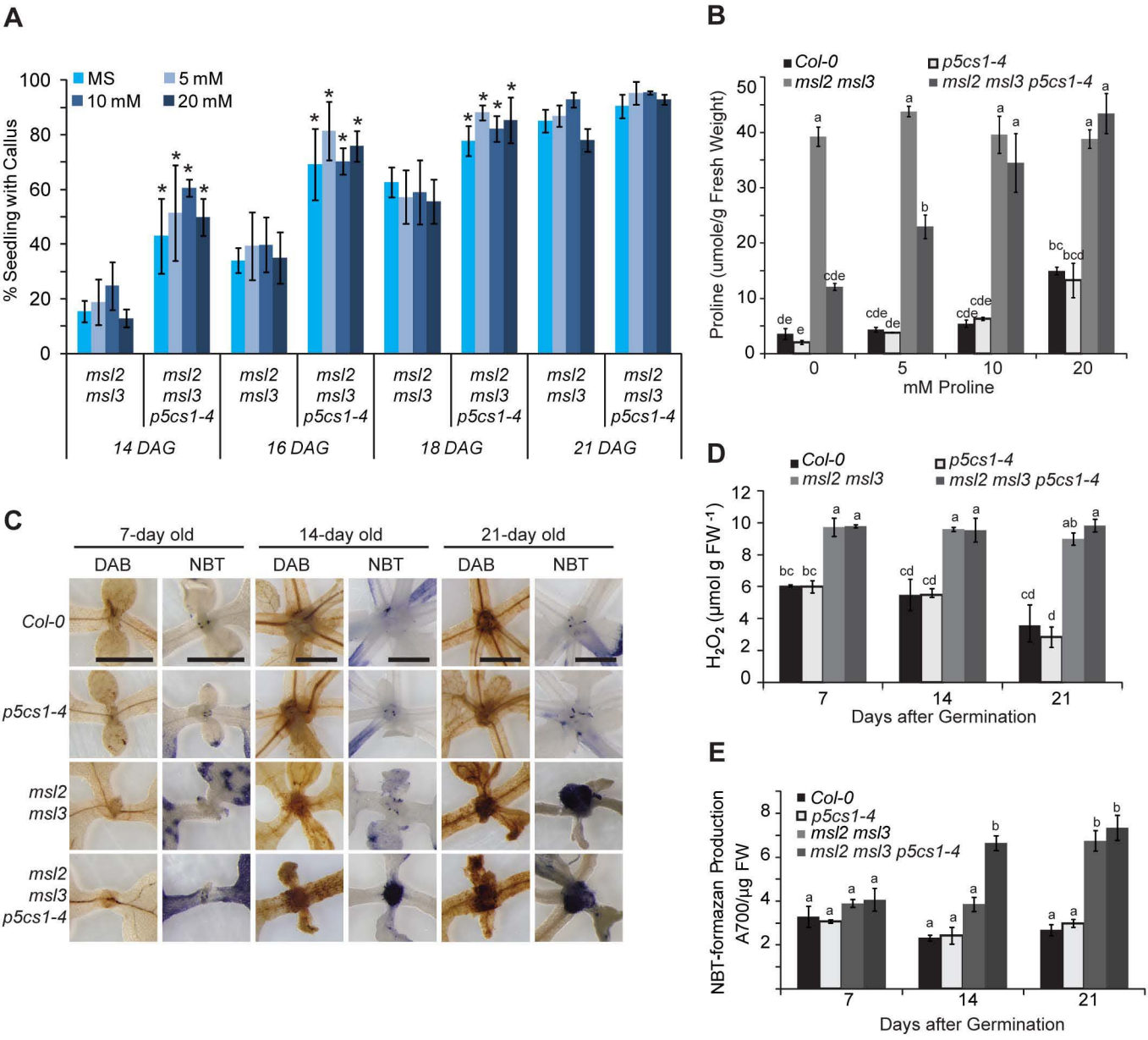
A
MS
5 mM
10 mM
20 mM
% Seedling with Callus
msl2 msl3
msl2 msl3 p5cs1-4
14 DAG
16 DAG
18 DAG
21 DAG
B
Col-0
p5cs1-4
msl2 msl3
msl2 msl3 p5cs1-4
Proline (umole/g Fresh Weight)
mM Proline
C
7-day old
14-day old
21-day old
DAB
NBT
Col-0
p5cs1-4
msl2 msl3
msl2 msl3 p5cs1-4
D
Col-0
p5cs1-4
msl2 msl3
msl2 msl3 p5cs1-4
H2O2 (µmol g FW-1)
Days after Germination
E
Col-0
p5cs1-4
msl2 msl3
msl2 msl3 p5cs1-4
NBT-formazan Production A700/µg FW
Days after Germination

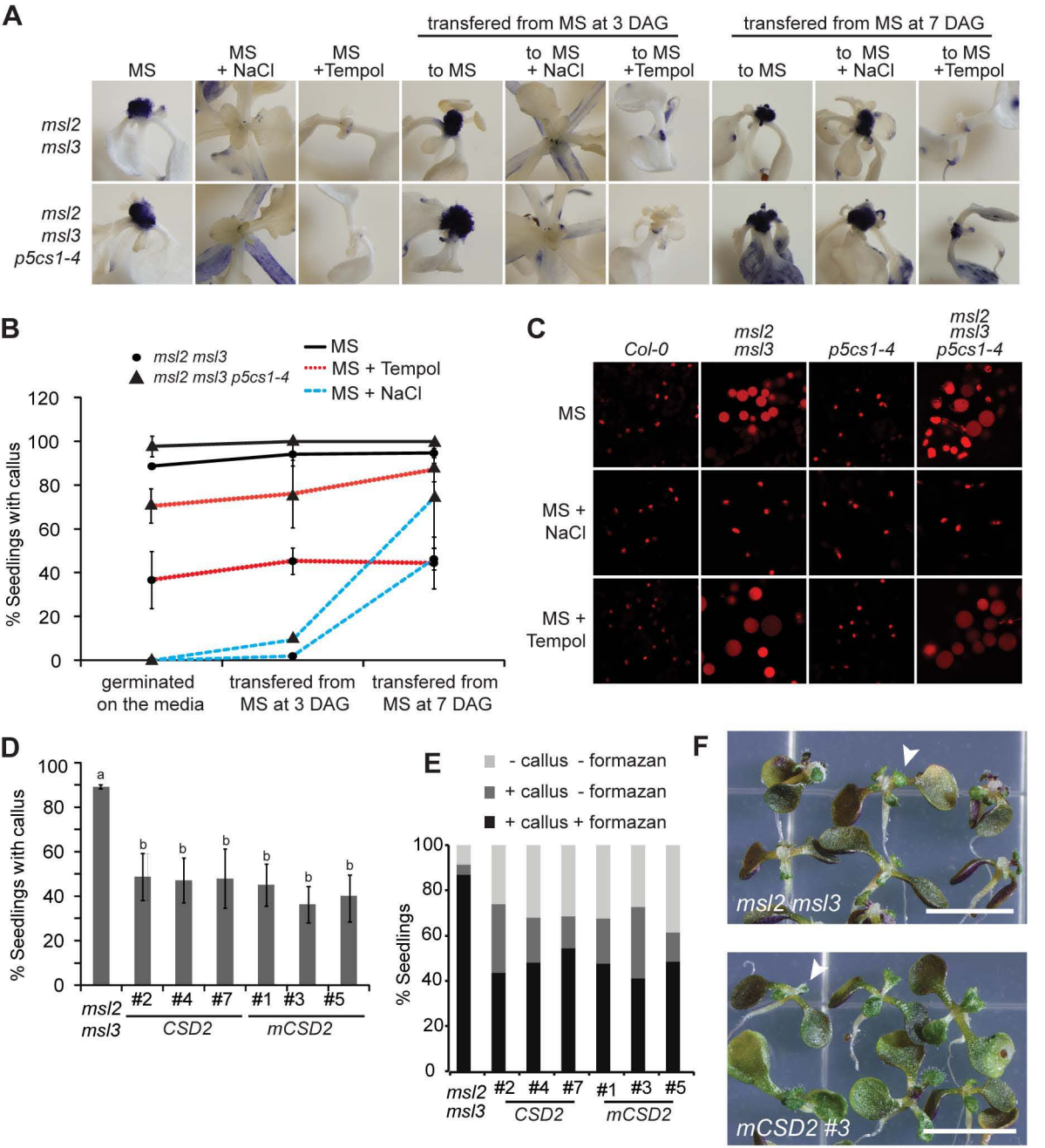
A
transfered from MS at 3 DAG
transfered from MS at 7 DAG
MS
MS + NaCl
MS +Tempol
to MS
to MS + NaCl
to MS +Tempol
to MS
to MS + NaCl
to MS +Tempol
msl2 msl3
msl2 msl3 p5cs1-4
B
msl2 msl3
msl2 msl3 p5cs1-4
MS
MS + Tempol
MS + NaCl
% Seedlings with callus
germinated on the media
transfered from MS at 3 DAG
transfered from MS at 7 DAG
C
Col-0
msl2 msl3
p5cs1-4
msl2 msl3 p5cs1-4
MS
MS + NaCl
MS + Tempol
D
% Seedlings with callus
msl2 msl3
#2 #4 #7
CSD2
#1 #3 #5
mCSD2
E
- callus - formazan
+ callus - formazan
+ callus + formazan
% Seedlings
msl2 msl3
#2 #4 #7
CSD2
#1 #3 #5
mCSD2
F
msl2 msl3
mCSD2 #3

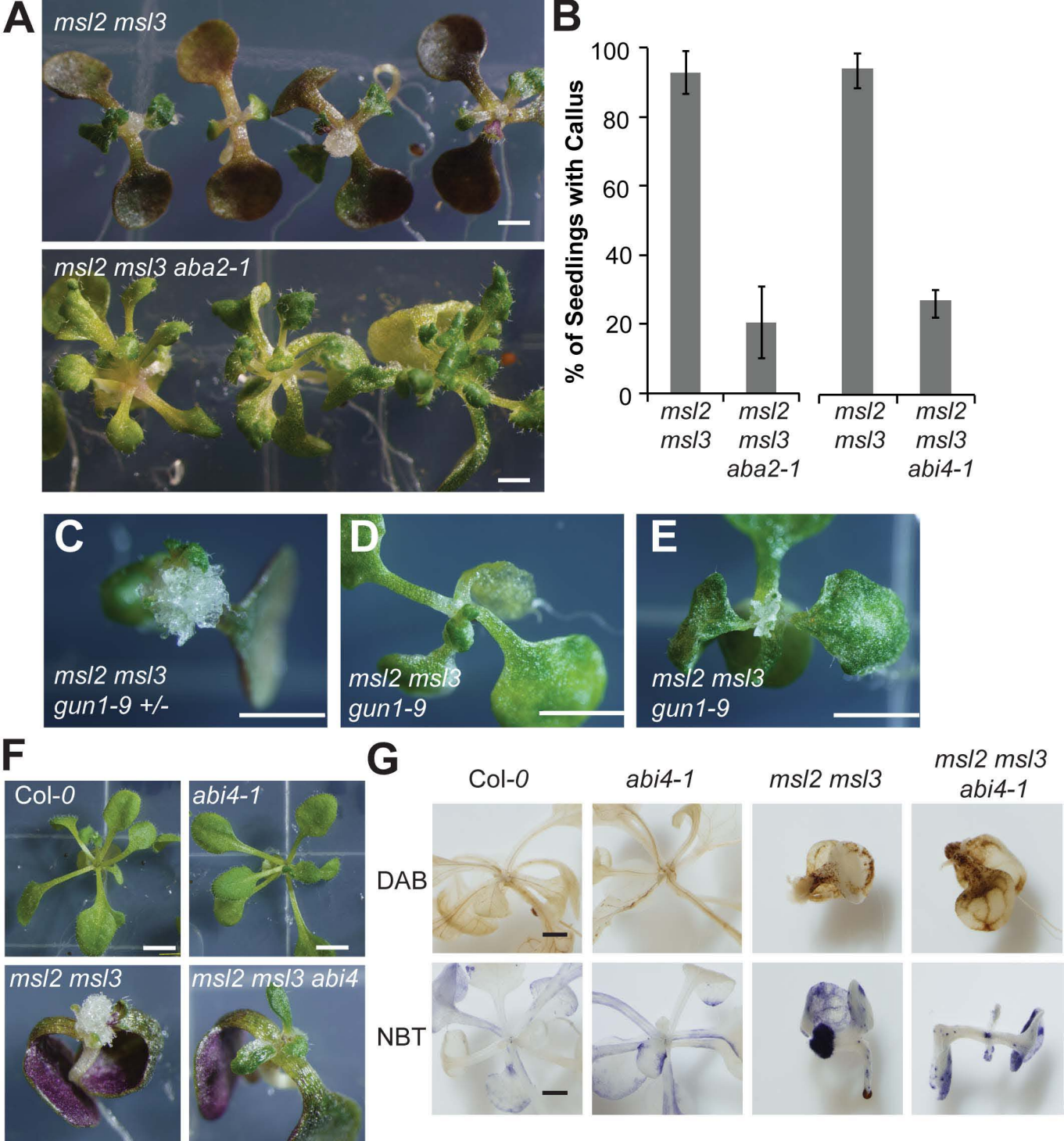
A
msl2 msl3
msl2 msl3 aba2-1
B
% of Seedlings with Callus
100
80
60
40
20
0
msl2 msl3
msl2 msl3 aba2-1
msl2 msl3
msl2 msl3 abi4-1
C
msl2 msl3 gun1-9 +/-
D
msl2 msl3 gun1-9
E
msl2 msl3 gun1-9
F
Col-0
abi4-1
msl2 msl3
msl2 msl3 abi4
G
Col-0
abi4-1
msl2 msl3
msl2 msl3 abi4-1
DAB
NBT

SUPPLEMENTARY FIGURE LEGENDS

Fig. S1. Additional analysis of callus production in *msl2 mls3* mutant seedlings. (A) Callus production is suppressed in *msl2 msl3* seedlings grown on MS supplemented with various osmotica. Top, percent of seedlings with visible apical callus after 3 weeks of growth on the indicated media. Bottom, individual seedling images. Scale bars are 5 mm. (B) *msl2 msl3* seedlings develop abnormal leaves after transfer from media containing osmotica to media without added osmotica. Bright field images of 21-day-old seedlings transferred at the indicated time points. Leaf notching is indicated by the white arrowheads.

Fig. S2. Additional transmission electron microscope (TEM) images of developing proplastids in the shoot apical meristem of 4-day-old wild type (A) and *msl2 msl3* mutants (B-D) seedlings. Size bar = 1 μm (A and C). (B) Proplastids are indicated (*), size bar = 10 μm. (C) Higher magnification images of the three proplastids marked with numbers in (B). Boxes in (C) are further magnified in (D) to show double membranes (white arrowhead). Size bar = 100 nm. Plastoglobules (PG), thylakoids (double black arrows).

Fig. S3. Characterization of callus production in *msl2 msl3* mutants. (A) Etiolated hypocotyl explants cultured on MS media containing the indicated concentrations of auxin (NAA) and cytokinin (kinetin). (B) Quantitative RT-PCR analysis of transcript levels of genes involved in callus production pathways in *msl2 msl3* mutants compared to the wild type. The average of three biological replicates (two technical replicates; $n \geq 25$ seedlings each) is presented. Error bars indicate SEM, $^{**}P<0.01$, $^{*}P<0.05$ (Student's *t*-test).

Fig. S4. Two *p5cs1* alleles exacerbate callus production in the *msl2 msl3* background. (A) Bright-field images of 21-day-old *msl2 msl3* and *msl2 msl3 p5cs1-4* mutants. Size bars, 5 mm. (B) Callus production at various time points after germination in *msl2 msl3*, *msl2 msl3 p5cs1-4*, and *msl2 msl3 p5cs1-1* seedlings. 5 plates of seedlings, $n > 10$ seedlings per plate, were analyzed per time point. (C) Bright-field images of *msl2 msl3 p5cs1-4* and *msl2 msl3 p5cs1-1* triple mutant seedlings at 21 DAG. Size bars, 5 mm.

Fig. S5. Additional images of *msl2 msl3 gun1-9 +/-* (A) and *msl2 msl3 gun1-9* triple mutant (B) siblings. Seedlings were grown for 21 days on solid media before imaging. Size bars, 2.5 mm.

35 **Fig. S6. Working model.** These results are consistent with a working model wherein plastid osmotic
36 stress impacts both a feedback loop regulating cell proliferation in the SAM (based on (Gaillochet et al.,
37 2015) and (Ikeuchi et al., 2013) and a plastid ROS-dependent retrograde signaling pathway (Leon et
38 al., 2012). Plastid osmotic stress leads to increased proliferation at the SAM and the production of
39 callus through increased CK levels and *WUS* expression and through an unknown nuclear
40 transcription program triggered by GUN1, ABA, and ABI4.
41

42 SUPPLEMENTARY METHODS

43

44 ***In Vitro* Callus Production.** Induction of *in vitro* callus production was performed as previously
45 described (Iwase et al., 2011). Etiolated hypocotyls were excised from mutant and wild type seedlings
46 4 days after germination. Mutant and wild type explants were cultured for 30 days side-by-side on MS
47 medium supplemented with Gamborg's vitamins, 2% glucose, 0.05% 2-(N-morpholino)ethanesulfonic
48 acid (MES), pH 5.8 with KOH, 0.8% phytoagar, and the indicated concentrations of NAA and kinetin.

49

50 **Quantitative RT-PCR.** Quantitative reverse transcription-PCR was performed as previously
51 described (Wilson et al., 2011). Primers used for gene expression analysis of *KPR and WIND* genes
52 were previously described (Iwase et al., 2011; Schiessl et al., 2014). The following primer pairs were
53 used to amplify *TDS1* (AGGCACTGCGGAATCTAGCAA and CTGGTCTGATTGTGGAAGGTCG) and
54 *TDS2* (CAGGTCAGCATCTCCTATGTCT and CCAAGATAGTTCTCACACCAGC) and *MAIL1*
55 (CTTGATCCTAGCAAGATCACTTGG and TGCCTCAGACACCTATCTGGA).

56

57 SUPPLEMENTARY REFERENCES

58

59 **Gaillochet, C., Daum, G. and Lohmann, J. U.** (2015). O cell, where art thou? The mechanisms of
60 shoot meristem patterning. *Curr Opin Plant Biol* **23**, 91-97.

61 **Ikeuchi, M., Sugimoto, K. and Iwase, A.** (2013). Plant callus: mechanisms of induction and
62 repression. *The Plant Cell* **25**, 3159-3173.

63 **Iwase, A., Mitsuda, N., Koyama, T., Hiratsu, K., Kojima, M., Arai, T., Inoue, Y., Seki, M.,**
64 **Sakakibara, H., Sugimoto, K., et al.** (2011). The AP2/ERF transcription factor WIND1
65 controls cell dedifferentiation in Arabidopsis. *Current Biology : CB* **21**, 508-514.

66 **Leon, P., Gregorio, J. and Cordoba, E.** (2012). ABI4 and its role in chloroplast retrograde
67 communication. *Frontiers in Plant Science* **3**, 304.

68 **Schiessl, K., Muino, J. M. and Sablowski, R.** (2014). Arabidopsis JAGGED links floral organ
69 patterning to tissue growth by repressing Kip-related cell cycle inhibitors. *Proceedings of the*
70 *National Academy of Sciences of the United States of America* **111**, 2830-2835.

71 **Wilson, M. E., Jensen, G. S. and Haswell, E. S.** (2011). Two mechanosensitive channel homologs
72 influence division ring placement in Arabidopsis chloroplasts. *The Plant Cell* **23**, 2939-2949.

73

74

A

% seedlings with apical callus (number of seedlings counted) when grown on the indicated media					
	MS	**MS + 82 mM NaCl**	**MS + 180 mM sucrose**	**MS + 180 mM mannitol**	**MS + 180 mM sorbitol**
Col-*0*	0 (186)	0 (48)	0 (99)	0 (61)	0 (153)
msl2 msl3	88 +/-10.8 (283)	4 +/- 5.9 (52)	5 +/- 1.8 (70)	39.1 +/- 16 (55)	35 +/- 18 (220)

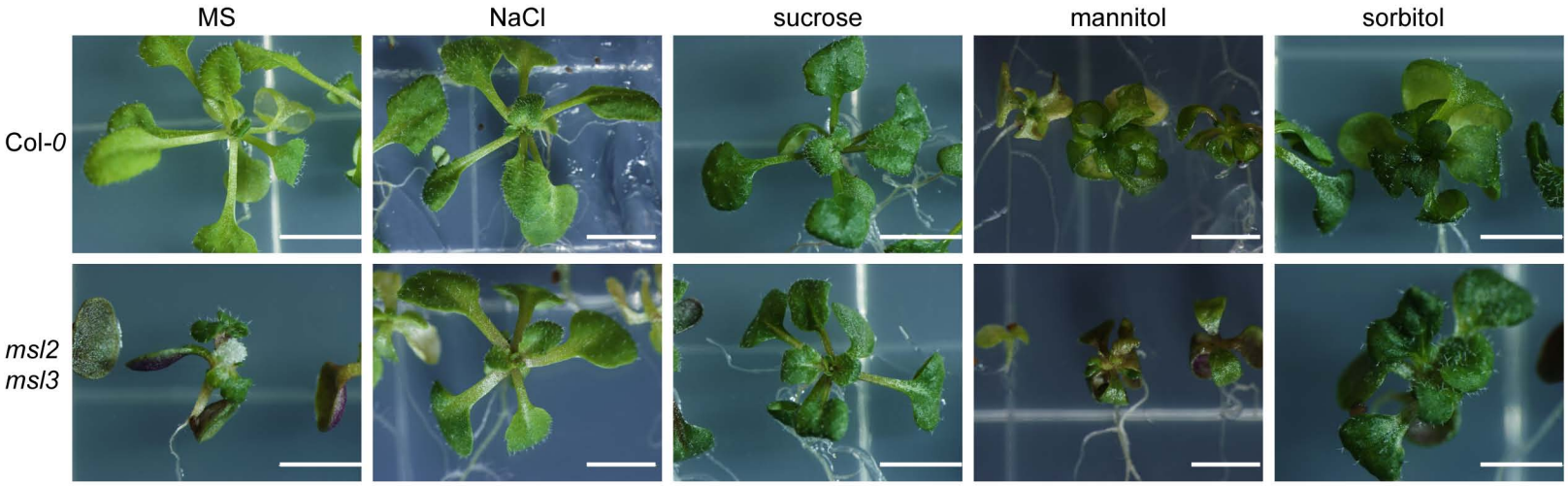

B

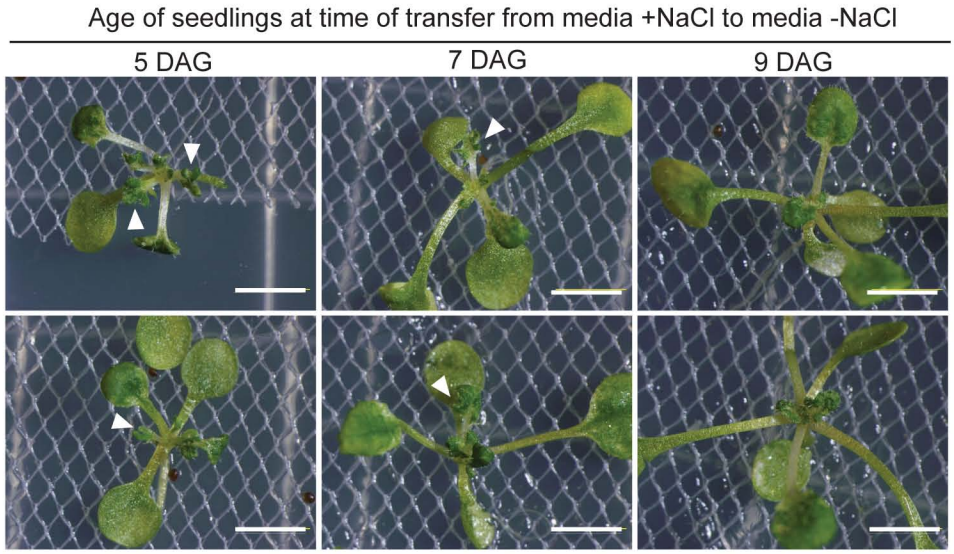

Fig. S1. Additional analysis of callus production in *msl2 mls3* mutant seedlings. (A) Callus production is suppressed in *msl2 msl3* seedlings grown on MS supplemented with various osmotica. Top, percent of seedlings with visible apical callus after 3 weeks of growth on the indicated media. Bottom, individual seedling images. Scale bars are 5 mm. (B) *msl2 msl3* seedlings develop abnormal leaves after transfer from media containing osmotica to media without added osmotica. Bright field images of 21-day-old seedlings transferred at the indicated time points. Leaf notching is indicated by the white arrowheads.

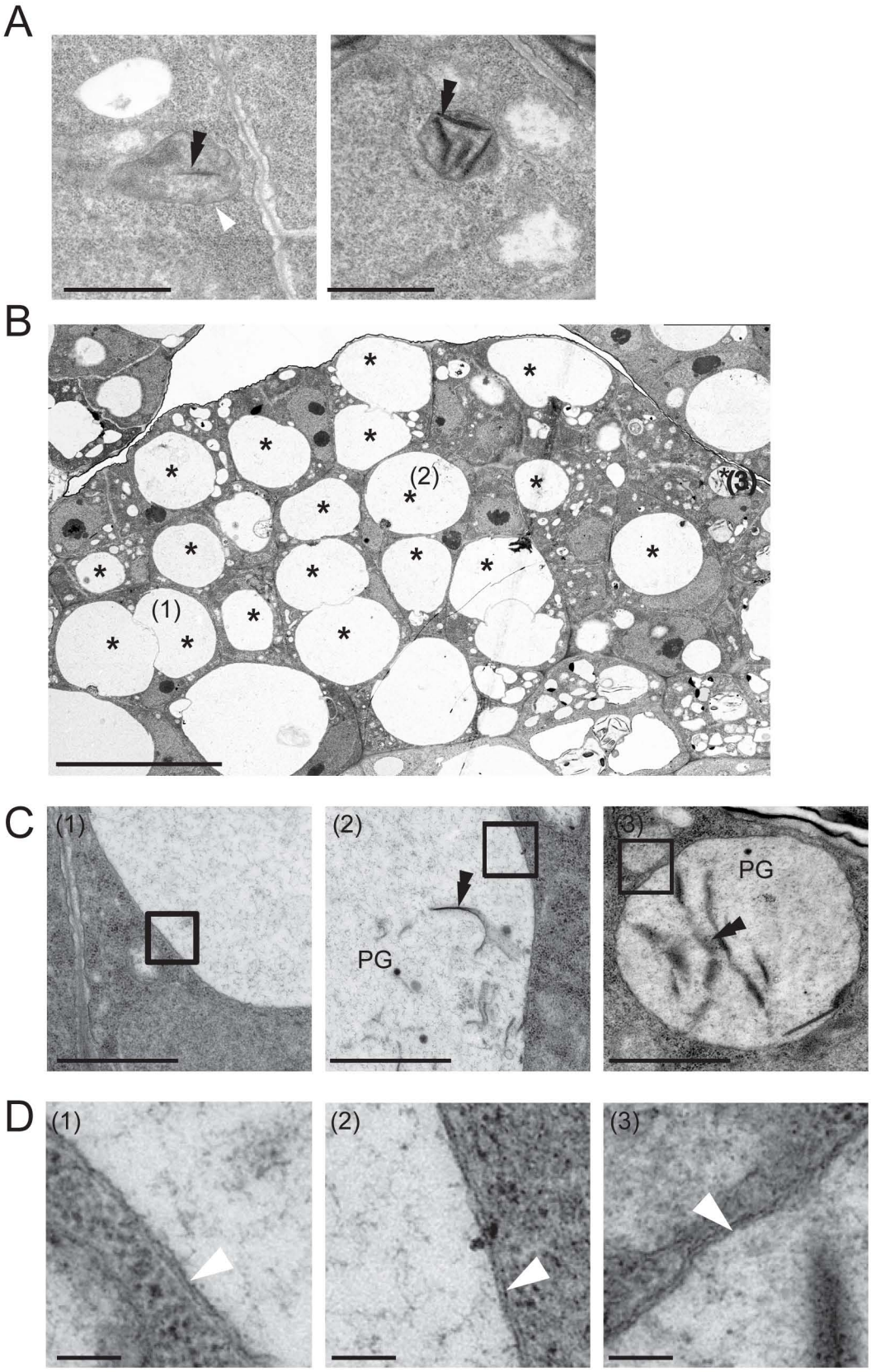

Fig. S2. Additional transmission electron microscope (TEM) images of developing proplastids in the shoot apical meristem of 4-day-old wild type (A) and *msl2 msl3* mutants (B-D) seedlings. Size bar = 1 µm (A and C). (B) Proplastids are indicated (*), size bar = 10 µm. (C) Higher magnification images of the three proplastids marked with numbers in (B). Boxes in (C) are further magnified in (D) to show double membranes (white arrowhead). Size bar = 100 nm. Plastoglobules (PG), thylakoids (double black arrows).

A

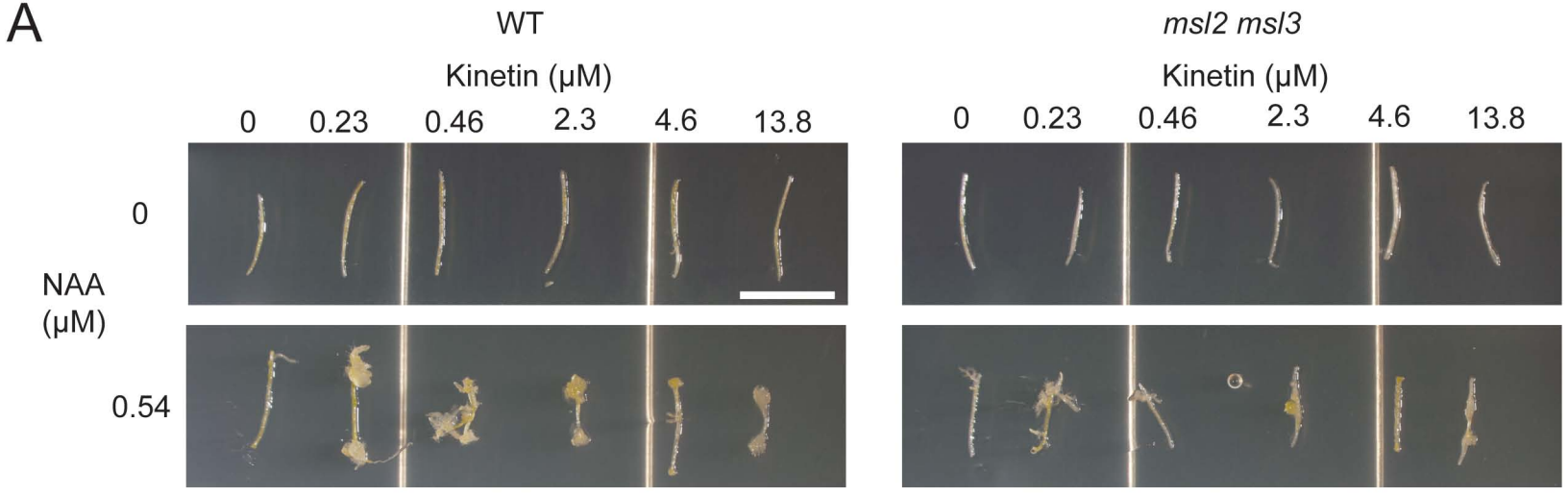
WT
msl2 msl3
Kinetin (μM)
0
0.23
0.46
2.3
4.6
13.8
NAA (μM)
0
0.54

B

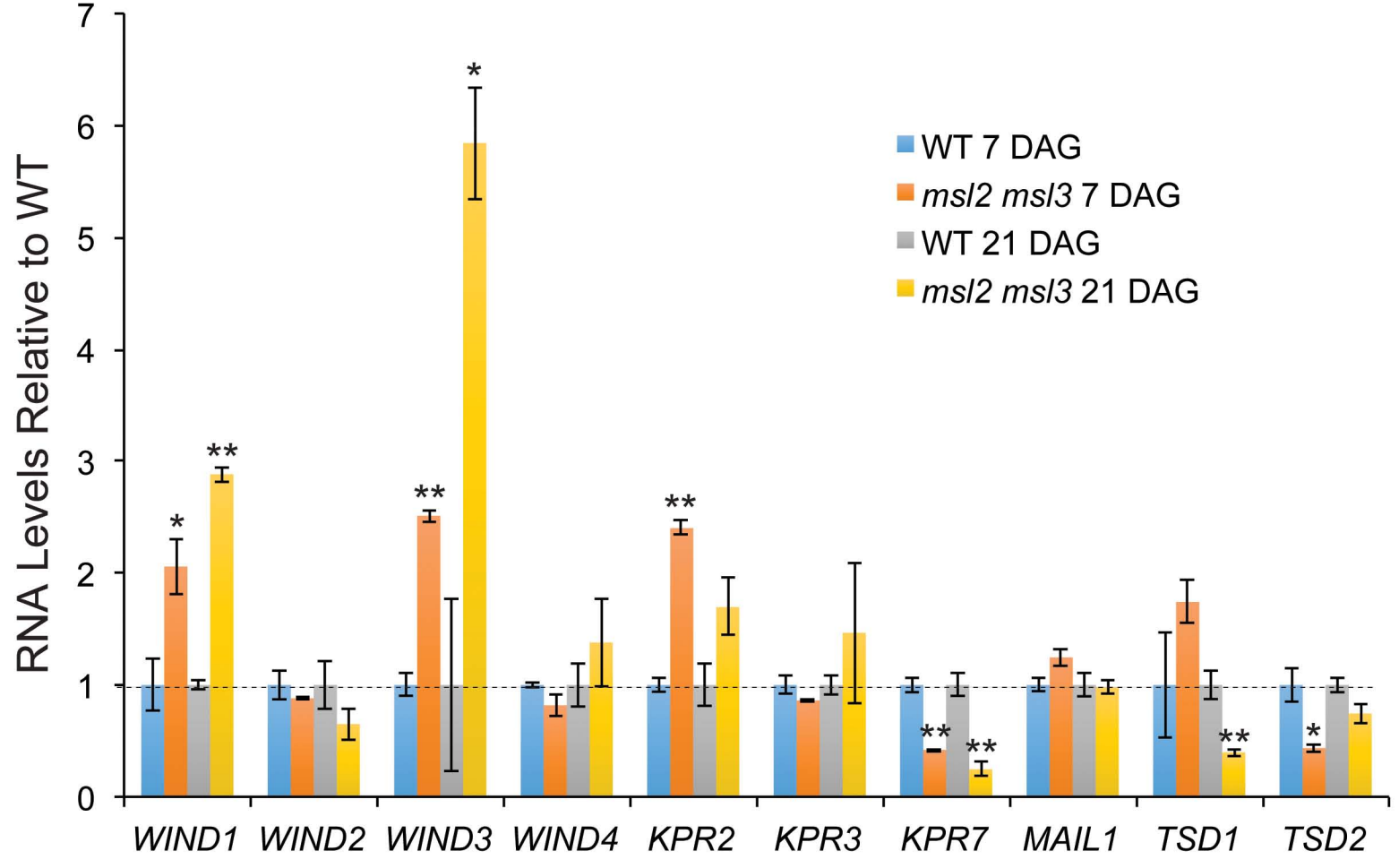
RNA Levels Relative to WT
0
1
2
3
4
5
6
7
WT 7 DAG
msl2 msl3 7 DAG
WT 21 DAG
msl2 msl3 21 DAG
WIND1
WIND2
WIND3
WIND4
KPR2
KPR3
KPR7
MAIL1
TSD1
TSD2

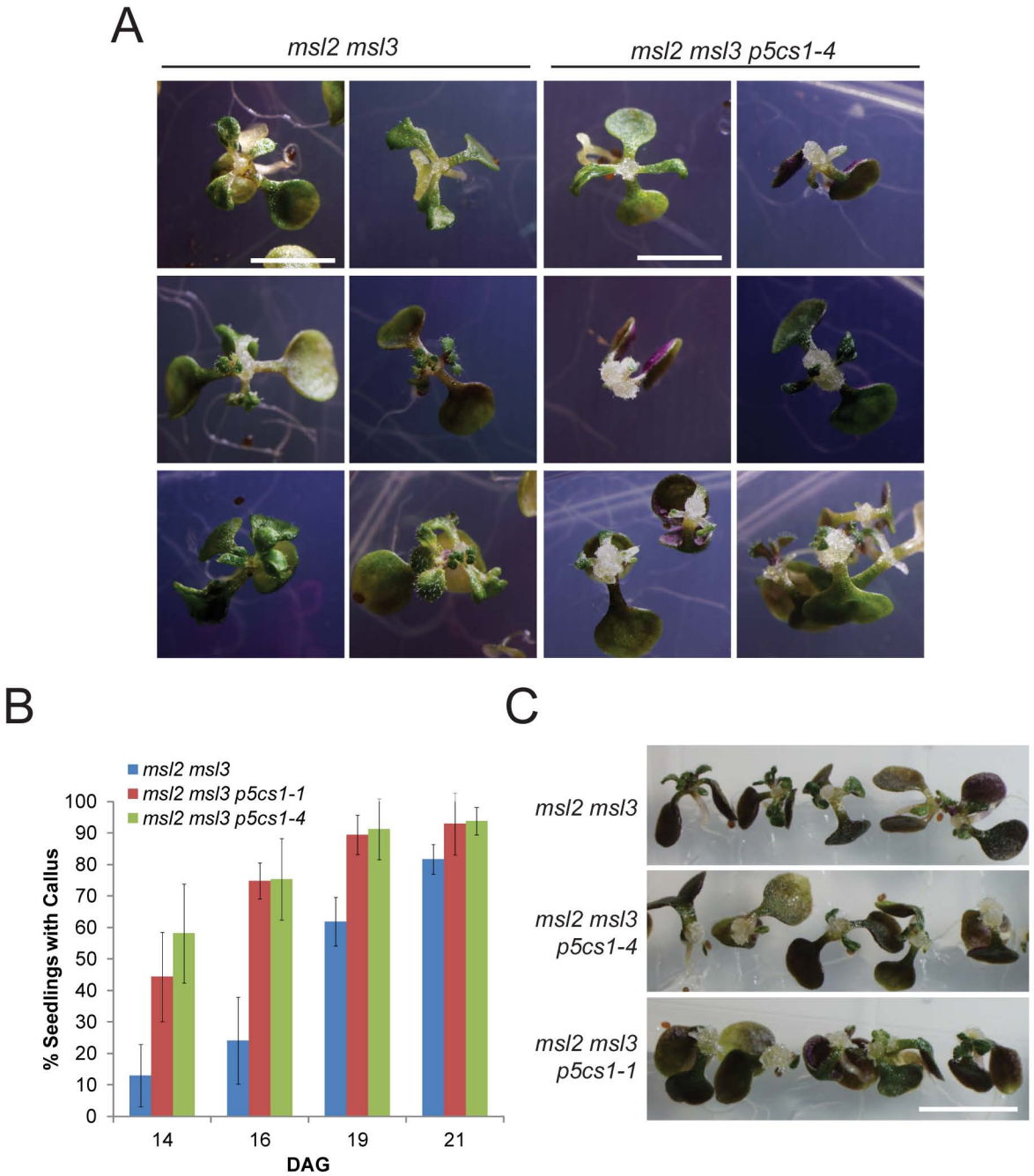

Fig. S4. Two *p5cs1* alleles exacerbate callus production in the *msl2 msl3* background. (A) Bright-field images of 21-day-old *msl2 msl3* and *msl2 msl3 p5cs1-4* mutants. Size bars, 5 mm. (B) Callus production at various time points after germination in *msl2 msl3, msl2 msl3 p5cs1-4,* and *msl2 msl3 p5cs1-1* seedlings. 5 plates of seedlings, n > 10 seedlings per plate, were analyzed per time point. (C) Bright-field images of *msl2 msl3 p5cs1-4* and *msl2 msl3 p5cs1-1* triple mutant seedlings at 21 DAG. Size bars, 5 mm.

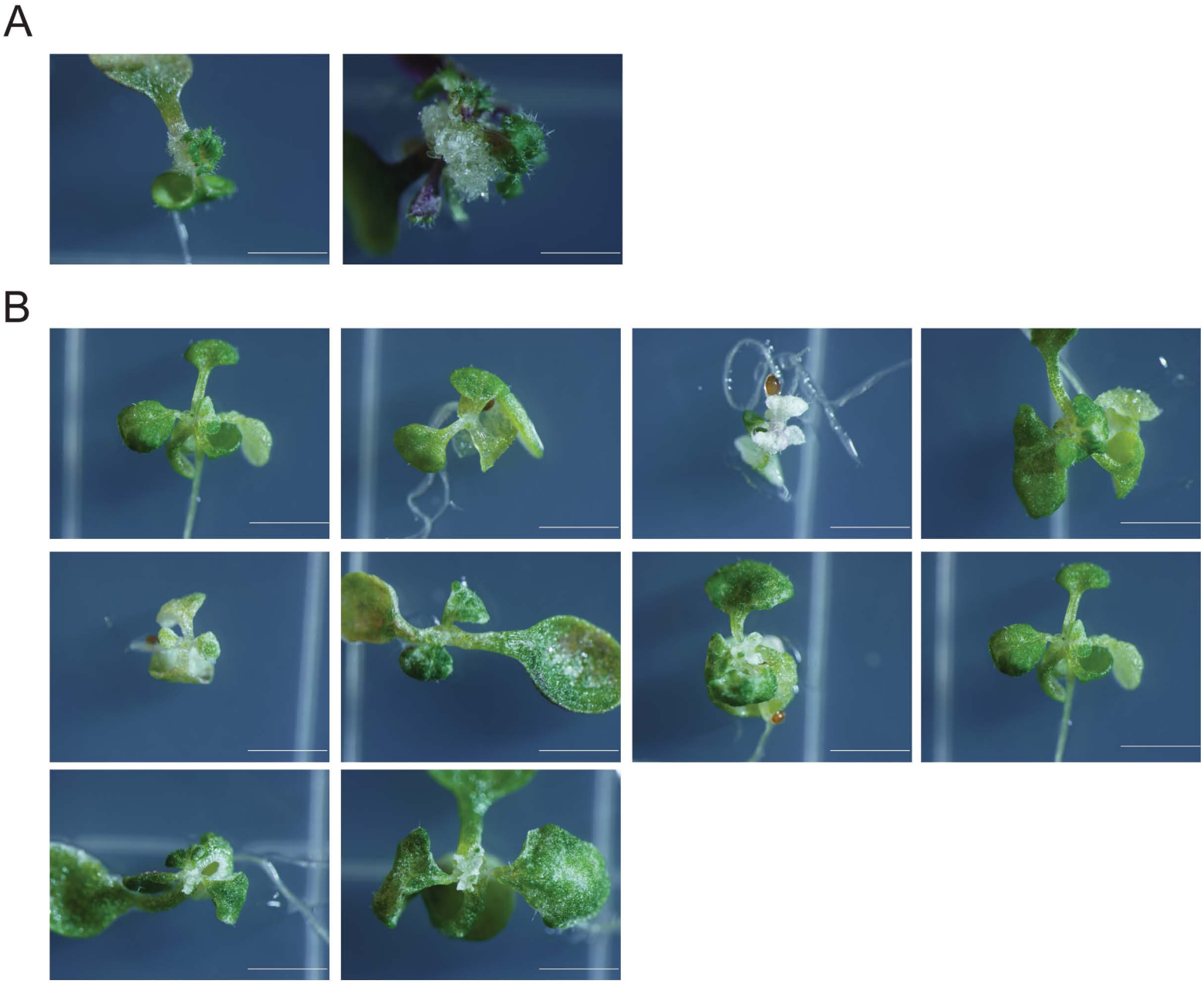

Fig. S5. Additional images of *msl2 msl3 gun1-9 +/-* (A) and *msl2 msl3 gun1-9* triple mutant (B) siblings. Seedlings were grown for 21 days on solid media before imaging. Size bars, 2.5 mm.

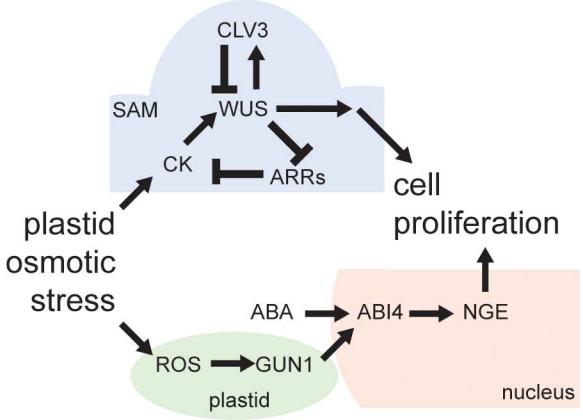

Fig. S6. Working model. These results are consistent with a working model wherein plastid osmotic stress impacts both a feedback loop regulating cell proliferation in the SAM (based on (Gaillochet et al., 2015) and a plastid ROS-dependent retrograde signaling pathway (Leon et al., 2012). Plastid osmotic stress leads to increased proliferation at the SAM and the production of callus through increased CK levels and *WUS* expression and through an unknown nuclear transcription program triggered by GUN1, ABA, and ABI4.